

**Characterization of Shear Stiffness and Cell Metabolism in  
Chondrocyte-Seeded Self-Assembling Peptide Hydrogel  
Scaffolds**

by

**Christina Marie Cosman**

B.S., Mechanical Engineering, Massachusetts Institute of Technology, 2001

Submitted to the Department of Mechanical Engineering  
in partial fulfillment of the requirements for the degree of

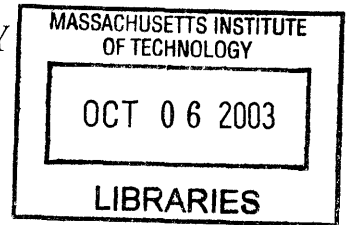
**Master of Science**

at the

**MASSACHUSETTS INSTITUTE OF TECHNOLOGY**

June 2003

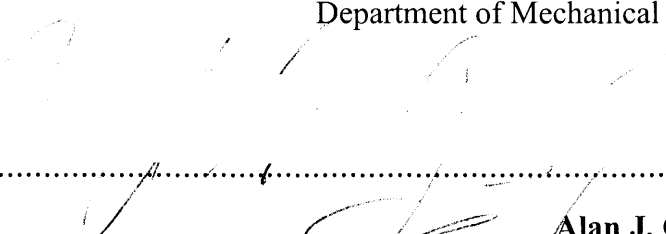
© Massachusetts Institute of Technology, 2003. All rights reserved.



Author .....

Department of Mechanical Engineering

Certified by .....

  
**Alan J. Grodzinsky**  
Professor of Biological, Electrical and Mechanical Engineering  
Thesis Supervisor

Accepted by.....

**Ain A. Sonin**  
Professor of Mechanical Engineering  
Chairman, Committee for Graduate Students

**ARCHIVES**

# Characterization of Shear Stiffness and Cell Metabolism in Chondrocyte-Seeded Self-Assembling Peptide Hydrogel Scaffolds

by

Christina Marie Cosman

Submitted to the Department of Mechanical Engineering  
on May 8, 2003 in Partial Fulfillment of the  
Requirements for the Degree of Master of Science

## ABSTRACT

Self-assembling KLD-12 peptide hydrogels have previously been established as suitable scaffolds for chondrocytes for the purpose of generating a three-dimensional, cartilaginous neo-tissue, which could potentially be implemented in the repair of *in vivo* chondral defects. Such tissue constructs have been shown to metabolically respond to dynamic compression by an increase in proteoglycan synthesis and glycosaminoglycan accumulation. For this thesis, modified chondrocyte-seeded, KLD-12 hydrogel constructs have been developed and evaluated for the characterization of age-dependent shear mechanical properties and metabolic response to shear loading.

Based on previous research, a new casting frame and technique were developed to create 2 mm thick, KLD-12 hydrogels for chondrocyte encapsulation. One day after casting, the total population in the hydrogel was 75-85% live, similar to the viability previously reported in 1.6 mm gels.

The equilibrium and dynamic shear stiffnesses of the constructs were determined over the course of 5-35 days post-casting. Methods for the application of pure shear deformation and the measurement of load response were similar to those previously used for cartilage explants. By Day 35, the average measured equilibrium and dynamic moduli were  $8.0 \pm 1$  kPa and  $67.7 \pm 21$  kPa, respectively. Thus, the construct stiffnesses were  $\sim 3$  orders of magnitude lower than explants in shear and  $\sim 1-2$  orders of magnitude lower than 1.6 mm constructs in confined compression.

A polysulfone (PSF) shear loading chamber was designed and fabricated to test the effect of dynamic shear deformation on metabolism of chondrocytes in 2 mm KLD-12 hydrogels. In contrast to the stimulatory result in cartilage explants, cyclic shear deformation caused a dramatic decrease in protein and proteoglycan incorporation in the KLD-12 constructs, compared to free-swell controls in culture plates. Notable increase in GAG loss in both loaded and unloaded chamber specimens suggested that chamber artifacts might have been responsible for these metabolic effects.

Validation studies of the shear chamber were conducted to determine the cause of biosynthetic suppression and GAG loss. The same phenomena occurred in a different chamber with similar geometry, so the biocompatibility of PSF was investigated, via several shielding experiments. However, PSF was not proven to be toxic to chondrocytes, and other factors in the chamber environment, such as gas diffusion or evaporation of culture medium, may have caused the catabolic effects.

Thesis Supervisor: Alan J. Grodzinsky

Title: Professor of Biological, Electrical and Mechanical Engineering

## Acknowledgements

I joined the Continuum Electromechanics Lab as a senior undergraduate at MIT and liked it so much that I decided to stay for another degree! Indeed, being a part of this lab has been a joy and a privilege. My sincerest thanks go to Alan Grodzinsky for giving me a place in the group and being a supportive and inspiring advisor. Al's guidance and good humor make the lab a most unique one, both in its accomplishments and its personality. Al's dedication to fostering interdisciplinary research helped me to bridge mechanical and biological engineering and to find a project that I was excited and challenged by.

Thanks also to all the lab members and visiting colleagues, who provided engineering knowledge, aid to my research, and an enjoyable work environment. It was wonderful to gain lasting friendships in addition to all those things. I am especially in debt to John Kisiday, a most attentive and encouraging mentor, who set a high standard for hard work and innovation in the lab and whose pioneering work with self-assembling peptide made my thesis possible.

Finally, I thank my dearest friends and family for guiding me in life and happiness. Their examples of excellence motivate me in every way.

Christina M. Cosman

May 8, 2003

# Contents

1	Introduction .....	12
1.1	Tissue engineering of cartilage .....	12
1.2	Articular Cartilage Composition.....	13
1.3	Self-Assembling Peptide Hydrogels .....	15
1.4	Shear Deformation of Cartilage.....	17
1.5	Thesis Objectives .....	19
2	Fabrication of Self-Assembling Peptide Hydrogels .....	21
2.1	Introduction.....	21
2.2	Methods.....	22
2.2.1	Cell Isolation.....	22
2.2.2	Preparation of Peptide Solution .....	22
2.2.3	Development of New Casting Frame.....	23
2.2.4	Hydrogel Casting .....	23
2.3	Results.....	25
2.4	Discussion .....	26
3	Evaluation of Shear Material Properties .....	27
3.1	Introduction.....	27
3.2	Methods.....	28
3.2.1	Specimen Preparation .....	28
3.2.2	Mechanical Testing.....	28
3.2.3	Shear Modulus Calculation.....	30
3.3	Results.....	31
3.4	Discussion .....	34

4	Effect of Dynamic Shear Loading on Chondrocyte Metabolism .....	36
4.1	Introduction.....	36
4.2	Methods.....	37
4.2.1	Development of Shear Loading Chamber for Hydrogel Disks.....	37
4.2.2	Shear Loading.....	38
4.2.3	Biochemical Analysis .....	40
4.3	Results.....	41
4.4	Discussion .....	43
5	Validation of Polysulfone Loading Chambers.....	45
5.1	Introduction.....	45
5.2	Methods.....	46
5.2.1	Chamber Comparison .....	46
5.2.2	Application of Poly-HEME Coating.....	47
5.2.3	Use of Teflon Sleeve.....	47
5.3	Results.....	48
5.4	Discussion .....	53
6	Summary and Future Work.....	55
6.1	Summary.....	55
6.2	Future Work.....	56
	Appendix A .....	59
	Appendix B .....	61
	References.....	66

## List of Figures

Figure 1	A schematic of the macromolecular structure of cartilage. ....	14
Figure 2	A molecular model of a single KLD-12 self-assembling peptide, exhibiting alternating hydrophilic (K, D) and hydrophobic (L) amino acid residues. ....	15
Figure 3	A scanning electron microscope image of the fiber structure of KLD-12. The fiber diameter is about 5-10 nm and the pore size ranges from 50-200 nm. ....	16
Figure 4	A schematic of cartilage in various states of deformation. Confined compression of cartilage induces fluid flow in addition to matrix deformation (B), whereas shear strain causes deformation only (C). ....	18
Figure 5	The components of the casting frame for fabrication of 2 mm thick hydrogel slabs. ....	23
Figure 6	The casting frame assembly. ....	24
Figure 7	The top and profile views of a 2 mm thick, chondrocyte-seeded KLD-12 hydrogel at Day 30. ....	25
Figure 8	The chamber for applying torsional shear deformation. Patches of fine grit sandpaper on the base and top platen prevent the hydrogel disks from slipping. ....	29
Figure 9	The intrinsic time-dependent stress relaxation response of a 30-day-old construct to successively applied ramp-and-hold shear strains. ....	32
Figure 10	The peak and equilibrium shear stress of 30-day-old constructs in response to ramp-and-hold shear strain. Both the peak and equilibrium shear stresses show a linear correlation with shear strain, with linear regression $R^2$ values of 0.99 and 0.97, respectively. ....	32

Figure 11 The average equilibrium shear modulus of constructs over time (n=5-11). From Day 5 to Day 35, the modulus increased to  $5.2 \pm 2$  kPa. ....33

Figure 12 A representative shear stress response of constructs to applied sinusoidal shear strain at 0.5 Hz. The ~ 17 degree difference in phase angle the between stress and strain curves demonstrates the viscoelastic behavior of the material, with elasticity being dominant over viscous effects. ....33

Figure 13 The average dynamic shear modulus of constructs over time (n=5-11). From Day 5 to Day 35, the modulus increased to  $67.7 \pm 21$  kPa.....34

Figure 14 A new shear polysulfone chamber for shear loading of the constructs. Notable features include adjustable-height porous platens, large well size, and top shear-axel attachment. ....38

Figure 15 The incubator-housed loading apparatus for the precise application of compression and shear. The shear chamber containing tissue constructs is wrapped to preserve sterility and mounted on the Incudyn. ....40

Figure 16 The  $^3\text{H}$ -proline and  $^{35}\text{S}$ -sulfate incorporation in dynamically sheared (Sh), shear chamber free-swell (Sh FS), and 12-well plate free-swell (FS) constructs. Incorporation in sheared samples was significantly lower ( $p < 0.001$ ) than in both other groups.....42

Figure 17 The  $^3\text{H}$ -proline and  $^{35}\text{S}$ -sulfate incorporation in dynamically sheared (Sh), shear chamber free-swell (Sh FS), and 12-well plate free-swell (FS) constructs. Compared to chamber free-swell, incorporation in the sheared disks was significantly higher ( $p < 0.05$ ), and both of those groups had significantly lower ( $p < 0.001$ ) incorporation than the 12-well free-swell controls. ....42

Figure 18 The Teflon sleeve to be inserted in the polysulfone loading chamber. ....48

Figure 19 The  $^3\text{H}$ -proline and  $^{35}\text{S}$ -sulfate incorporation in compression chamber free-swell (Cm FS), shear chamber free-swell (Sh FS), and 12-well plate free-swell (FS) constructs. Incorporation in the compression chamber was significantly lower ( $p < 0.001$ ) than in the shear chamber,



	and both were much lower ( $p < 0.001$ ) than controls in the 12-well plate. ....	49
Figure 20	The $^3\text{H}$ -proline and $^{35}\text{S}$ -sulfate incorporation in shear chamber free-swell (Sh FS), Poly-HEME-coated shear chamber free-swell (Sh Coat), 12-well plate free-swell (FS), and Ploy-HEME-coated 12-well plate free-swell constructs. Proline and sulfate incorporation levels were slightly lower ( $p < 0.001$ and $p < 0.05$ , respectively) in uncoated than in coated shear chamber samples. Incorporation in all shear chamber samples was significantly lower ( $p < 0.001$ ) than that in coated and uncoated 12-well controls.....	50
Figure 21	The GAG content in the culture medium of shear chamber free-swell (Sh FS), Poly-HEME-coated shear chamber free-swell (Sh Coat), Teflon sleeve free-swell (Tef FS), and 12-well plate free-swell (FS) constructs. After 1 day in culture, shear chamber samples lost approximately 3 times more GAG than coated chamber disks. New medium from the second day in culture contained approximately twice as much GAG in the uncoated than in coated chamber samples. GAG levels in the Teflon sleeve medium remained similar to those of 12-well controls on both days.....	51
Figure 22	The $^3\text{H}$ -proline and $^{35}\text{S}$ -sulfate incorporation in Poly-HEME-coated shear chamber free-swell (Sh Coat), shear chamber free-swell (Sh FS), Teflon sleeve free-swell, and 12-well plate free-swell (FS) constructs. Only the proline incorporation in the coated chamber samples was slightly lower ( $p < 0.05$ ) than uncoated; sulfate incorporation levels between the two were not significantly different. Incorporation in Teflon sleeve and 12-well control samples was approximately 2-fold higher than in coated and uncoated chamber samples. ....	51
Figure 23	The $^3\text{H}$ -proline and $^{35}\text{S}$ -sulfate incorporation in shear chamber free-swell (Sh FS), Poly-HEME-coated shear chamber free-swell (Sh Coat), Teflon chamber insert free-swell (Sh Tef), and 12-well plate free-swell (FS) constructs. Incorporation was higher ( $p < 0.05$ and	

p<0.001, respectively) in both coated chamber and Teflon insert samples, compared to uncoated chamber samples. ....52

Figure 24 The GAG content in the culture medium of shear chamber free-swell (Sh FS), Teflon sleeve free-swell (Tef FS), Poly-HEME-coated shear chamber free-swell (Sh Coat), and 12-well plate free-swell (FS) constructs. After 1 day in culture, chamber free-swell medium had .....52

Figure A-1 The casting frame window component, made of stainless steel (quantity 1). ....59

Figure A-2 The casting frame U-clamp component, made of stainless steel (quantity 2). ....60

Figure B-1 The shear loading chamber base component, made of polysulfone (quantity 1). ....62

Figure B-2 The shear loading chamber top component, made of polysulfone (quantity 1). ....63

Figure B-3 The alternate view of the shear loading chamber top component shown in Figure B-2. ....64

Figure B-4 A polysulfone platen-holder for a porous shear loading platen (quantity 6). ....65

# List of Tables

Table 1	Dynamic shear loading protocols .....	39
---------	---------------------------------------	----

# Chapter 1

## Introduction

### 1.1 Tissue engineering of cartilage

While the occurrence of severe articular cartilage injuries and resulting debilitating conditions, such as osteoarthritis, are common among adults [1, 2], there is a lack of fully effective treatments to restore normal functionality to the affected joints. Current clinical and trial treatments include joint replacement [3], joint debridement, soft tissue grafting, osteochondral transplantation, allo- and autografting, and chondrocyte transplantation [4]. Though some of these procedures are promising, none has yet been able to produce long-term restoration of damaged articular surfaces and load-bearing joint function [4].

Tissue engineering techniques provide enormous potential for surpassing the efficacy of current treatments of cartilage defects. A prevalent paradigm in tissue engineering-based repair of articular surfaces is filling the defect volume with a three-dimensional cell-seeded biomaterial scaffold, which acts as a “living implant” that will integrate with the surrounding tissue and mimic its biochemical and mechanical properties. Many researchers are working to optimize the scaffold materials, morphologies, and culture conditions that will yield a superior neo-tissue. Potential materials may be composed of synthetic polymers [6-8] or natural fibers [9-12], both of which have unique advantages and disadvantages. Synthetic materials allow for customized processability, degradability, material strength, architecture, and

permeability, whereas natural materials may possess innate cell interaction capabilities and more inflammatory inertness [13]. Additionally, these scaffolds may be modified with bioactive molecules, such as growth factors or adhesion proteins, which may help to govern their interaction with cells [4].

In conjunction with the scaffold material, the *in vitro* culture conditions of the cell-scaffold construct may play an important role in its performance *in vivo*. Culture of such neo-tissues prior to implantation allows the embedded cells to adjust to their new extracellular environment and resume their normal activity of extracellular matrix (ECM) synthesis, leading to the formation of new cartilage-like material within the scaffold. Over time, the mechanical strength of the construct increases, because of new ECM formation, and thus more closely resembles the mechanical properties of native cartilage [8, 14, 15]. This pre-culturing may enhance the success of constructs as implants by enabling them to better withstand physiological loads due to joint motion and weight bearing. Certain schemes of *in vitro* mechanical stimulation of constructs have been shown to stimulate chondrocyte biosynthesis, thereby augmenting their ECM production and accelerating tissue stiffening [16-21, 24]. Load conditioning may be a of great advantage to the development of tissue engineered implants, because it would reduce the *in vitro* culture time required for the constructs to attain physiological stiffness before implantation, thus reducing the risk of pre-transplant contamination.

## **1.2 Articular Cartilage Composition**

To engineer a tissue that is intended to mimic articular cartilage, one must understand the biochemical composition, physiological function, and mechanical behavior of the native tissue. Articular cartilage, which lines all the articulating joint surfaces of the body, has unique molecular constituents, which govern its lubricative and load-bearing functions. The tissue consists predominantly of a porous, solid matrix, made up of collagen fibrils (~20% wet weight, 50-65% dry) and proteoglycans (~5% wet weight, 25-35% dry), water (~75% wet weight), chondrocytes (2-10% by volume), and non-collagenous proteins, lipids and glycoproteins (~10% dry weight) [25-28, 30]. The

schematic in Figure 1 shows the main tissue components. The network of collagen fibrils, primarily type II, provides the tissue with tensile and shear strength and retains the proteoglycan molecules, whose negatively charged glycosaminoglycan side chains help to maintain osmotic swelling in the tissue, lending it compressive stiffness [31]. The spacing of collagen fibrils and the concentration of proteoglycans determine cartilage porosity [25].

Chondrocytes are responsible for the production and turnover of these ECM molecules, via interactions with endogenous and exogenous soluble mediators and through the influence of mechanical forces [25, 32]. Given the proper culture conditions, chondrocytes will continue to generate ECM molecules, but their rates of biosynthesis depend on the specific biochemical and biomechanical environment. In the case of a severe cartilage defect *in vivo*, the avascular, alymphatic, and aneural nature of cartilage limits its ability to generate normally functioning repair tissue [33-35]. Damaged cartilage loses its load-bearing and lubricative capacity, thereby disrupting normal joint function and potentially leading to more serious degenerative conditions such as osteoarthritis [37]. For this reason, finding an effective tissue engineering solution to cartilage repair would be extremely important.

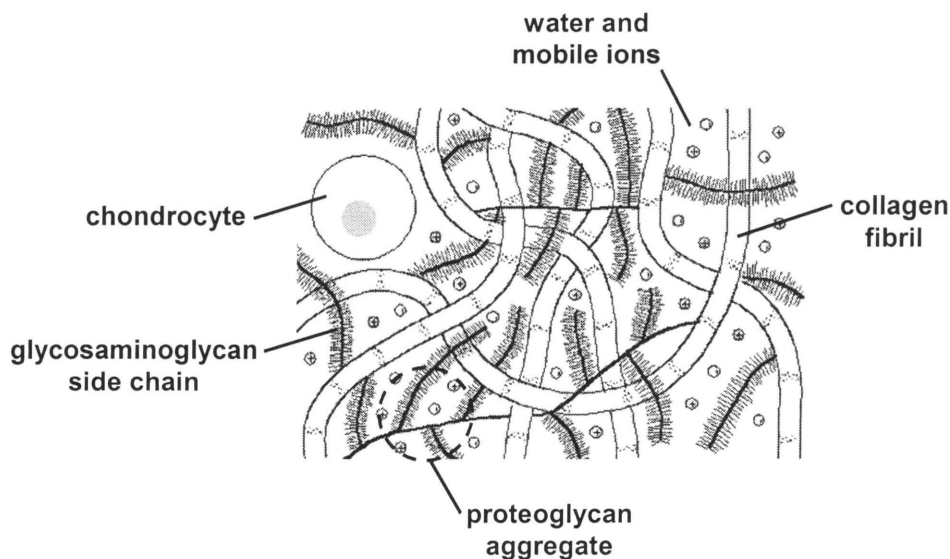


Figure 1: A schematic of the macromolecular structure of cartilage.

### 1.3 Self-Assembling Peptide Hydrogels

The self-assembling peptide hydrogel is a promising candidate for a cartilage tissue engineering scaffold material [15, 24, 35]. The primary structure of these peptides consists of short amino acid chains with repeating sequences of alternating hydrophobic and hydrophilic side groups, as shown in Figure 2 [38, 39]. This electronegativity scheme causes aqueous solutions of type I classified peptides to rapidly form  $\beta$ -sheet fibrils when exposed to physiologic ionic strengths and pH levels [32, 40, 41]. Photographed in Figure 3, the fiber diameter is fairly regular in the range of 5-10 nm [35] with a network pore size of 50-200nm [41]. The small fiber thickness, compared to most other polymer fibers [15] and the large amount of void space (> 99% water content) [32, 46] provide ample room for intercellular interaction and neo-matrix deposition. A major advantage of this type of peptide for use in biomaterial design is that different peptide sequences can be selected and easily synthesized, allowing one to tailor the material to specific applications [32], such as the engineering of cartilage.

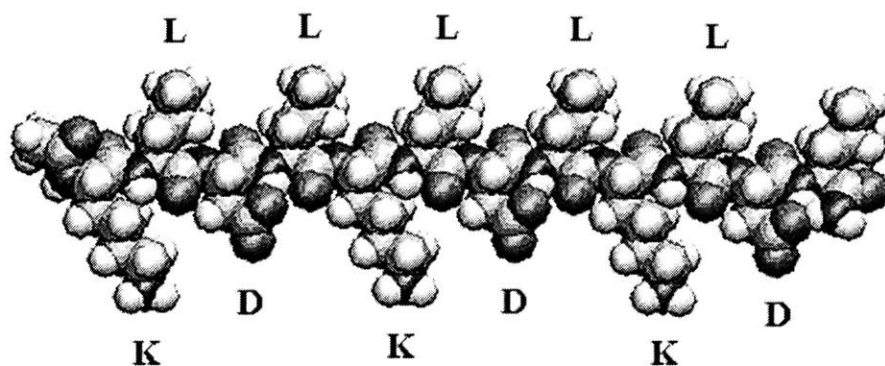
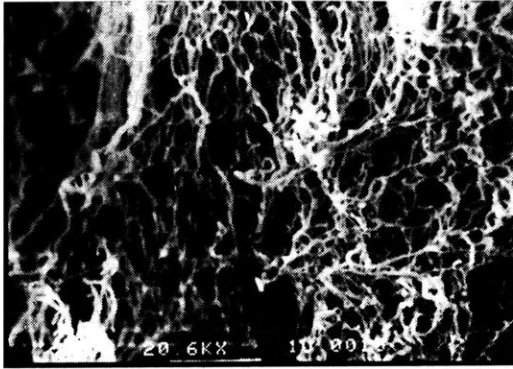


Figure 2: A molecular model of a single KLD-12 self-assembling peptide, exhibiting alternating hydrophilic (K, D) and hydrophobic (L) amino acid residues.



**Figure 3:** A scanning electron microscope image of the fiber structure of KLD-12. The fiber diameter is about 5-10 nm and the pore size ranges from 50-200 nm.

Several different peptide sequences have been tested for various cell culture applications [42, 43]. Specifically, the KLD-12 sequence has been investigated for chondrocyte compatibility and found to foster phenotypic stability and proliferation of chondrocytes encapsulated within its hydrogels, as well as cartilaginous ECM production and retention [15]. KLD-12 is a twelve amino acid, type I peptide with consecutive repeats of Lysine, Leucine, Aspartic Acid, and Leucine, resulting in a +, 0, -, 0 charge pattern under conditions near physiologic pH. Although the innate biochemical composition and mechanical strength (<1 kPa equilibrium modulus) of KLD-12 hydrogels [15] are very different from those of cartilage, over time, the cell-scaffold constructs increasingly resemble the natural tissue, both biochemically and mechanically, because of cumulative chondrocyte deposition and scaffold retention of new ECM [15].

From a tissue engineering perspective, this type of hydrogel is superior to previous materials used for chondrocyte encapsulation [5, 17-19, 44, 45], in that it offers greater flexibility for molecular design, which could influence scaffold biodegradability, *in vivo* tissue integration, cell signaling, and biomolecular tethering [15]. Furthermore, synthetic scaffolds have less risk of carrying biological pathogens or contaminants than biologically derived scaffolds materials would [46].



## 1.4 Shear Deformation of Cartilage

The material behavior of cartilage stems from the interaction of its solid and fluid components. Classification of cartilage as a poroviscoelastic material takes into account its “biphasic nature”, namely the flow of interstitial fluid relative to the solid ECM, whose intrinsic behavior is viscoelastic [47-49]. ECM viscoelasticity is thought to arise from several molecular dynamics, including the mechanics of individual collagen molecules, inter-fibril sliding, and relative collagen-proteoglycan motion [50]. One model is that bundled type II collagen molecules behave like parallel springs in tension, storing elastic energy, whereas viscous sliding between cross-linked collagen fibrils and between fibrils and proteoglycans dissipates energy nonlinearly [51, 52]. Another model explains matrix viscoelasticity by lumping all collagen and proteoglycan molecules into their respective networks, each with its own nonlinear stress-strain behavior [29]. The poroviscoelastic model is most relevant to the case of compressive loading (Figure 4B), in which the solid matrix deforms immediately, resulting in increased fluid pressure within the tissue and forcing the interstitial fluid to flow to a region of lower pressure [53]. However, in the case of macroscopic shear deformations, such as simple and pure shear (Figure 4C), there is approximately no volumetric change in the tissue. Thus, intra-tissue fluid flow and pressure gradients would be negligible, and the material behavior could be described by the viscoelastic deformation of the solid matrix only [54-56].

Because of this phenomenon, shear loading of cartilage decouples matrix deformation from interstitial fluid flow and allows one to assess the effects of deformation alone on mechanical behavior and cellular processes [57]. Several experiments to characterize the shear mechanical properties of cartilage explants have confirmed the tissue’s viscoelastic behavior under simple shear deformation [53, 57-59]. The tissue demonstrates a time-dependent stress relaxation response to a constant strain deformation, which is characteristic of viscoelastic behavior.

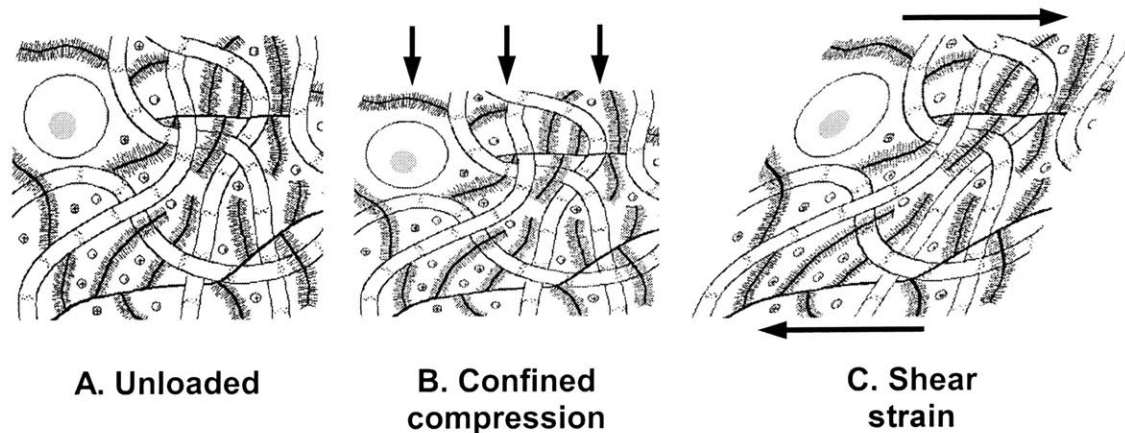


**Figure 4: A schematic of cartilage in various states of deformation. Confined compression of cartilage induces fluid flow in addition to matrix deformation (B), whereas shear strain causes deformation only (C).**

Shear loading has also been applied to cartilage explants to test its effect on chondrocyte metabolism. These studies have been motivated by the goal of understanding how the physiological forces, both compressive and shear, that articular cartilage experiences *in vivo* influence its material properties. Previous studies have showed that dynamic compressive loading of explants increased protein and proteoglycan synthesis in explants, hypothesizing that interstitial fluid flow, streaming potential, and mechanical deformation of cells and ECM were responsible [60, 61]. Dynamic shear loading of explants could elucidate which of those stimuli plays the largest regulatory role, by causing deformation in the absence of fluid flow [57]. Indeed, several studies have shown that certain dynamic shear loading protocols can increase protein and proteoglycan synthesis, suggesting that tissue deformation without fluid flow has this regulatory effect [35, 57, 62].

These findings in explants raise the question of whether similar shear loading protocols could have the same stimulatory effect on tissue engineered cartilage constructs. The analogy between explants and artificial tissue has been extensively investigated with compression loading schemes, and results have consistently been transferable [17-21, 24]. Corresponding studies employing dynamic shear loading have not been well documented, although Waldman et al. recently reported that intermittent cyclic shear deformation of cartilaginous tissue formed *in vitro* could significantly increase its equilibrium modulus and collagen and proteoglycan content, relative to

unloaded control levels [62]. This finding supports the need for exploring the effects of dynamic shear conditioning on other forms of engineered cartilage, such as KLD-12 constructs, which is a main objective of this thesis.

## 1.5 Thesis Objectives

Self-assembling KLD-12 hydrogels have previously been established as suitable environments for hosting chondrocytes in order to generate a three-dimensional, cartilaginous neo-tissue, which could be implemented in the repair of chondral defects *in vivo* [15, 21, 24]. The motivation and background studies leading to the pioneering work with chondrocyte-seeded KLD-12 hydrogels is presented in Chapter 1 of this thesis. Kisiday et al. have developed fabrication and culture techniques for these unique hydrogels that are salubrious for chondrocyte viability, phenotypic stability, and biosynthesis. Furthermore, timelines of the histology, new matrix accumulation, and compressive mechanical properties of the construct have been documented, demonstrating its biochemical and biomechanical similarity to natural cartilage.

In order to more fully characterize the mechanical integrity of this novel material, its shear material properties must be measured. Chapter 2 describes the considerations and processes used to create chondrocyte-seeded KLD-12 hydrogels that are suitable for shear loading. The fabrication and composition of constructs for shear loading are primarily the same as those previously used for compression tests, but the increased thickness of these gels causes some slight changes in experimental materials and procedures. The shear equilibrium and dynamic moduli of these constructs could then be evaluated, and the details of these procedures are presented in Chapter 3.

Determining the effects of dynamic loading schemes on the metabolism of chondrocytes encapsulated in KLD-12 hydrogels requires imposition of several different kinds of loading that the constructs might experience *in vivo*, including both compression and shear. Certain dynamic compression duty cycles have been shown to increase proteoglycan synthesis in the constructs, compared to free-swell controls, paralleling similar stimulatory results in explants [21, 23, 24]. A logical next step is to dynamically

shear the constructs in hopes that the explant analogy also holds for this type of loading. If dynamic shear could augment protein synthesis in the constructs, as it did in explants [57], then shear conditioning effects could be complementary to dynamic compression induced proteoglycan stimulation. Combined loading modes could potentially build a stronger construct in a shorter time, thereby minimizing *in vitro* culture time and allowing earlier *in vivo* implantation. Hence, Chapter 4 describes preliminary attempts at shear conditioning of chondrocyte-seeded KLD-12 hydrogels. For these studies, a new loading chamber was manufactured, various loading protocols were tested, and subsequent biochemical assays were performed.

Results that dramatically opposed our hypothesis of anabolic stimulation due to dynamic shear prompted a series of studies to evaluate the adequacy of the new loading chamber as a bioreactor for this tissue-engineered material. Chapter 5 provides background on this type of bioreactor chamber for cartilaginous tissue culture and reports on various validation experiments to elucidate its influence on the metabolism of chondrocyte-seeded KLD-12 hydrogels.

A summation of the findings from all studies in this thesis and suggestions for future experiments and directions are included in Chapter 6.

## Chapter 2

# Fabrication of Self-Assembling Peptide Hydrogels

### 2.1 Introduction

Kisiday et al. have successfully pioneered the development of self-assembling KLD-12 hydrogels as a scaffold for cartilage tissue engineering [15, 21-24]. The cylindrical geometry of these constructs was designed to have 1.6 mm height, mimicking the thickness of *in vivo* articular cartilage, and 12.5 mm diameter to provide sufficient area for compressive loading and subsequent sample analysis. The functional requirements for the constructs used in this thesis are slightly different, so the hydrogel geometry needed to be altered. A thicker gel was required for shear loading because a larger aspect ratio (thickness to diameter) would minimize the slippage of samples relative to chamber surfaces during application of simple shear deformation. A new casting frame was machined, such that it would yield 2 mm thick hydrogel slabs with slightly larger length and width, to allow the extraction of nine 12.5 mm diameter specimens. All experimental materials and procedures remained unchanged from those previously used [15, 24], except for the gelation time and casting frame disassembly. Because of the larger volume of cell-peptide solution needed to fill this new casting frame, the gelation process required a minimum of one hour to complete, to allow sufficient time for salt diffusion and peptide self-assembly. Resulting hydrogels also tended to stick to the flanking sheets of agarose-coated filter paper, so more sensitive frame removal was necessary to separate an intact slab.

## **2.2 Methods**

### **2.2.1 Cell Isolation**

Immature bovine chondrocytes were extracted according to a previously developed protocol, which is briefly described here [74]. Cartilage slices were taken from the femoral chondyles and femoropatellar grooves of 1-2 week old calves within a few hours of slaughter. These slices were then manually chopped into fine pieces and transferred to a DMEM (Gibco, high glucose), 10% FBS (Hyclone), and pronase (Sigma) solution for 3 hours of incubation, after which the tissue was rinsed twice with 1x PBS and placed into a DMEM, 10% FBS, and collagenase (Worthington, type 2) solution overnight. The next day, the tissue-collagenase solution was mixed via pipetting and allowed to incubate for another 1.5 hours to complete digestion. The chondrocytes were then filtered using 40  $\mu\text{m}$  cell strainers, twice rinsed in 1x PBS, and re-suspended in low-serum, DMEM-based culture medium supplemented with 1% ITS (Sigma Chemical) [15, 24]. A sample of cell solution was analyzed under a microscope for cell viability and concentration using Trypin Blue staining. The solution was pipetted into volumes corresponding to a hydrogel seeding density of 30 million cells per ml and stored at  $-20^{\circ}\text{C}$  until use.

### **2.2.2 Preparation of Peptide Solution**

This protocol for preparing the peptide solution for hydrogel formation is based on a similar procedure developed by Kisiday, et al. [15]. KLD-12 stock was custom synthesized (SynPep Corp., Dublin, CA) and procured in non-sterile, lyophilized form. Volume for a peptide hydrogel concentration of 3.6 mg peptide per ml of cell solution was weighed and dissolved in a 10% sucrose solution by alternating between sonication and vortex agitation. The peptide-sucrose solution was subsequently sterile-filtered using a 20  $\mu\text{m}$  syringe filter and sonicated until use to prevent peptide aggregation.

### 2.2.3 Development of New Casting Frame

The design of a new casting frame for production of 2 mm thick hydrogel slabs was derived from the original frame used by Kisiday [24]. New design parameters of this frame include a thicker, 2 mm frame stock and a slightly larger, 1.7 in<sup>2</sup> casting window. Stainless steel frame components were custom fabricated by water-jet cutting and their machine drawings are included in the Appendix A. The frame components and mesh spacer sheets are displayed in Figure 5.

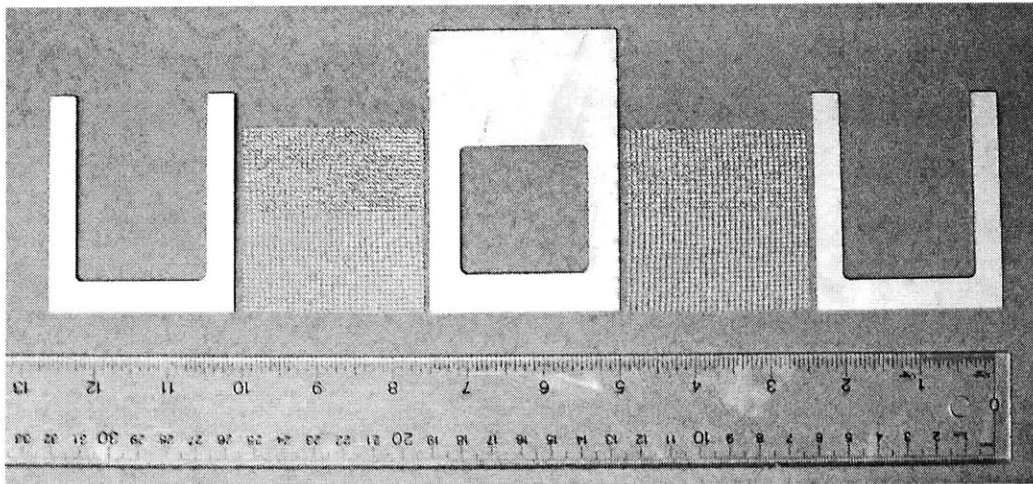
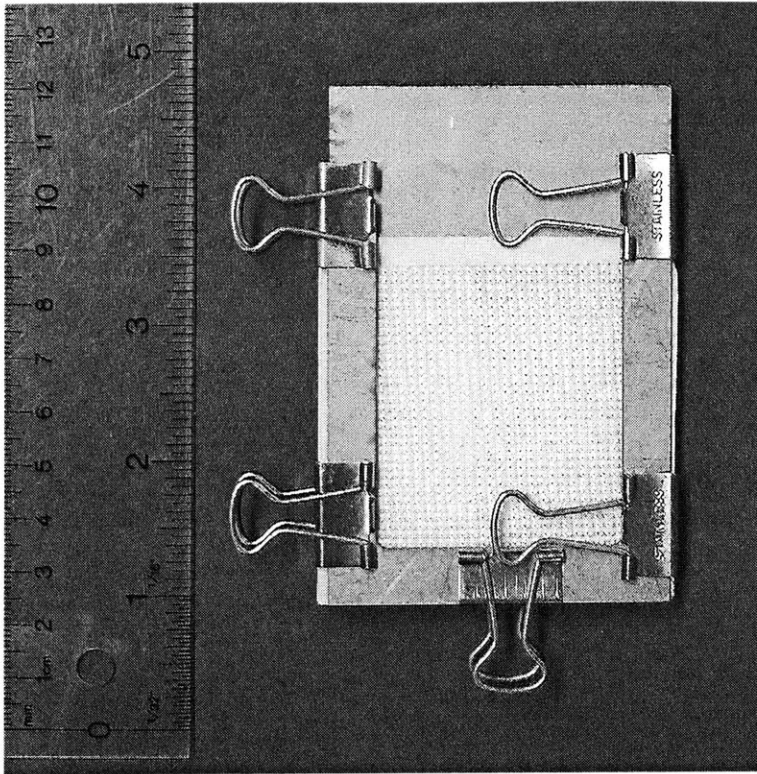


Figure 5: The components of the casting frame for fabrication of 2 mm thick hydrogel slabs.

### 2.2.4 Hydrogel Casting

This procedure for fabricating chondrocyte-seeded KLD-12 hydrogels was based on the one used by Kisiday et al. [15, 24]. The appropriate volume of cell solution one hydrogel was centrifuged at 1800 rpm for 10 minutes, during which custom cut pieces of filter paper (Whatman #1) were coated on one side with 0.6% agarose solution and refrigerated until use. During the last minute of centrifuging, the casting frame components were assembled as shown in Figure 6.



**Figure 6: The casting frame assembly.**

Medium was aspirated from the chondrocyte pellet and the cells were resuspended in a solution of 10% sucrose and 5 mM HEPES buffer, the volume of which was 10% of the final hydrogel volume. The peptide-sucrose solution was drawn into a syringe to 90% of the final hydrogel volume and swiftly injected on top of the cell-sucrose solution. The resulting solution was lightly vortexed and immediately injected into the casting frame window. The entire assembly was then placed in a 1.4x PBS bath to initiate peptide self-assembly. After a minimum time of 1 hour, the frame was removed from the bath and held parallel to the ground while the outer-most U-frame pieces were disassembled. The top mesh piece was slid away and the underlying filter paper was peeled away very slowly to eliminate any spots where the hydrogel may have been stuck to it. Both the filter paper and the mesh were replaced so that the frame could be flipped over and the mesh and paper on the other side could be removed. The window piece was carefully lifted away from the hydrogel and the remaining filter paper supporting the hydrogel was placed in a petri dish and supplied with 23ml of low-serum, 1% ITS-supplemented medium. The filter paper was then removed using sterile forceps and the hydrogel was



placed in an incubator. After 4-5 days in culture, hydrogels slabs were cored with a custom, stainless steel, 12.5 mm diameter punch to produce nine geometrically identical hydrogel disks, which were transferred to 12-well culture plates with 2.5 ml of medium per well. A mature sample is shown in Figure 7.

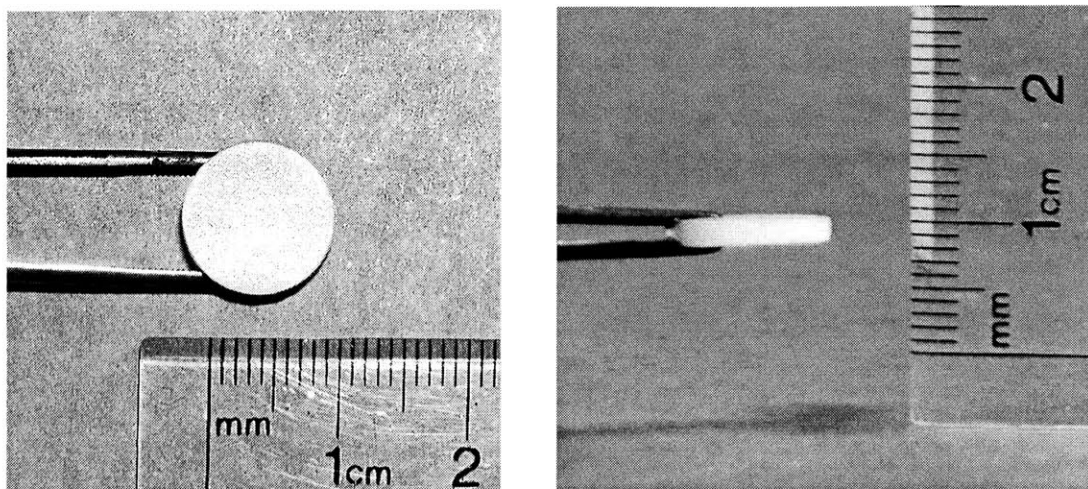


Figure 7: The top and profile views of a 2 mm thick, chondrocyte-seeded KLD-12 hydrogel at Day 30.

## 2.3 Results

Casting with the new casting frame produced 2 mm thick, flat slabs of chondrocyte-seeded KLD-12 hydrogels, similar to those previously created with a 1.6 mm frame [15, 24]. After fine-tuning of the frame removal process, fully intact gels could be extracted consistently without sticking to the agarose-coated filter paper. For a 3.6 mg/ml peptide concentration dissolved in a 10% sucrose solution, the minimum time for peptide self-assembly upon immersion in a PBS bath was determined to be 60 minutes, compared to 25 minutes for a 1.6 mm gel [24]. The day after casting, cell viability in the gel was approximately  $80\% \pm 5\%$  live cells, according to a red/green biofluorescence assay. This result is consistent with that of 1.6 mm hydrogels. Under microscope inspection, chondrocytes also appeared to be evenly distributed throughout the area of the slab.

## **2.4 Discussion**

The successful production of thicker hydrogels was important to the thesis goal of subjecting them to various types of shear deformation, because a gel with a greater thickness-to-diameter ratio would cause less error in stress response due to frictional sliding between hydrogel and chamber surfaces. It also has positive implications for creation of three-dimensional cell-seeded scaffolds for tissue engineering, which may require unique tissue construct geometries. Constructs with more complex morphology could potentially be made by employing different casting frame geometries or even by stacking two or more slabs on top of each other immediately after casting, allowing biochemical and mechanical integration between them.

## Chapter 3

# Evaluation of Shear Material Properties

### 3.1 Introduction

The success of tissue engineered cartilage for use as an *in vivo* implant depends largely on its ability to withstand the physiological forces present in the joint environment [15, 24]. Articular cartilage experiences a combination of compression, tension, hydrostatic pressure, pure and simple shear, and fluid-induced shear forces *in vivo* [29, 35, 64]. These forces not only challenge the tissue's load bearing and joint lubricating functions, but aid its homeostasis as well [57, 64]. If a three-dimensional tissue construct is to fill an articular cartilage defect *in vivo*, its mechanical properties, such as compressive and shear moduli, must first be assessed *in vitro* and compared to those of natural cartilage. The compressive moduli of 1.6 mm thick chondrocyte-seeded KLD-12 hydrogels have previously been measured at time points ranging from 0 to 26 days in culture. By Day 26, the equilibrium modulus was found to be 10% and the dynamic modulus was 5% of the corresponding moduli of native cartilage [15]. For this thesis, the equilibrium and dynamic shear moduli of these constructs have been measured in 5-day intervals, spanning up to 35 days in culture, beginning from the casting date. The shear loading performed here can provide a basis for comparing the mechanical integrity and behavior of the construct material to those corresponding properties of articular cartilage.

## **3.2 Methods**

### **3.2.1 Specimen Preparation**

Chondrocyte-seeded KLD-12 hydrogels were removed from culture at various time points ranging from Day 5-35, where the casting date was Day 0, and placed in 1x PBS solution. A media sample and the wet weight of each specimen were taken for subsequent GAG analysis. The hydrogel thickness was measured and used to calculate the applied shear strain.

### **3.2.2 Mechanical Testing**

The method of shear mechanical testing of the chondrocyte-seeded KLD-12 hydrogels is similar to that used by Jin et al. for testing of cartilage explants [58]. Mechanical deformation was applied to specimens using an Incudyn apparatus, which can prescribe precise axial and torsional displacements and forces via a computer interface [75]. Samples were placed in a previously used loading chamber (Figure 8), whose base was fixed to the rotational platform of the Incudyn and whose concentrically aligned lid was fastened to an axially actuated post on the machine. Very fine grit sandpaper affixed to both the base and the contact platen of the lid prevented specimen slippage during shear loading.

A hydrogel was placed in the center of the chamber base and the lid was lowered until it met the sample surface, which was designated as the axial and rotational zero position. The chamber well was then filled with 1x PBS solution and the sample was allowed to equilibrate for 3 minutes, after which the protocol for measuring the equilibrium shear modulus was initiated. A 15% compressive offset was applied by a 50  $\mu\text{m/s}$  ramp-and-hold for the duration of 3 minutes. Next, a shear ramp was applied with the same velocity until 1.5% of the sample thickness was reached, and this displacement was held for the rest of 3 minutes. This ramp-and-hold sequence was repeated 3-4 times

consecutively, after which the platen was returned to its rotational zero position, where the hydrogel equilibrated again for 3 minutes.

Following equilibration, the protocol for determining the dynamic shear modulus began. Sinusoidal shear deformation with an amplitude of 0.8% of sample thickness and a frequency of 0.5 Hz was applied for 10 seconds (~ 5 cycles) and the platen returned to absolute zero. Data was recorded for all steps at a sampling rate of 256 samples/s by a Dynamic Acquisition Program linked to the Incudyn.

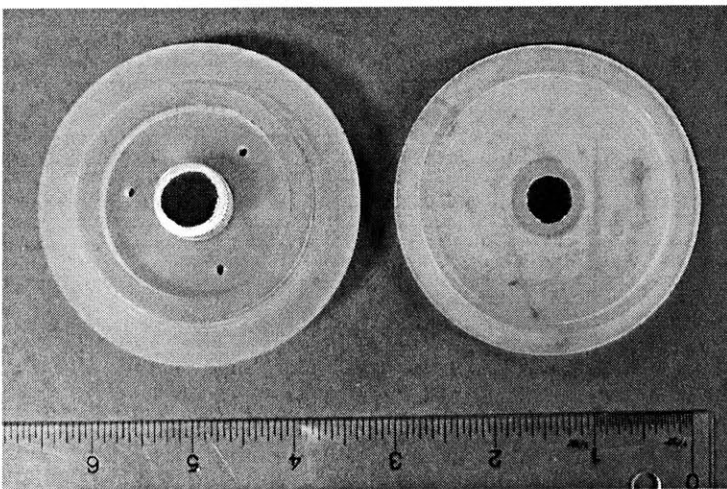
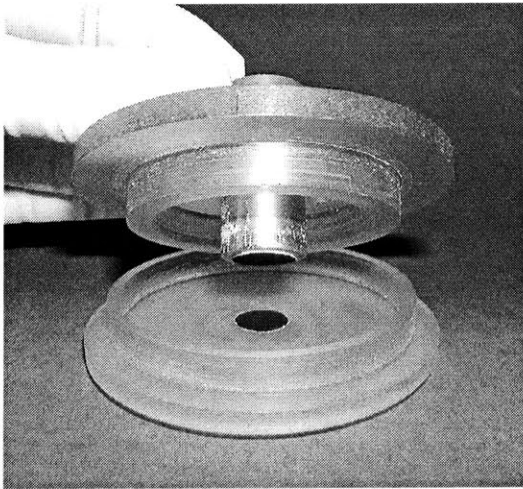


**Figure 8: The chamber for applying torsional shear deformation. Patches of fine grit sandpaper on the base and top platen prevent the hydrogel disks from slipping.**

### 3.2.3 Shear Modulus Calculation

The equilibrium modulus was calculated from a plot of the relaxed shear stress versus the applied shear strain. The shear strain at the outer edge of the hydrogel is given by

$$\gamma = \frac{\theta R}{h}, \quad (1)$$

where  $\theta$  is the applied rotational angle,  $R$  is the hydrogel radius, and  $h$  is the hydrogel thickness. For these experiments, the shear strain was prescribed as a percentage of the sample thickness. The sample radius and thickness were input, so the torsional displacement to apply could be determined. The shear stress response at the outer edge of the hydrogels was computed from the relation

$$\tau = \frac{TR}{J}, \quad (2)$$

where  $T$  is the measured torque and  $J$  is the polar moment of inertia, which for this hydrogel geometry is

$$J = \frac{1}{2} \pi R^4. \quad (3)$$

Hence, the equilibrium modulus could be calculated by finding the slope of the shear stress after stress-relaxation versus the corresponding shear strain that was applied to produce that stress.

The dynamic shear modulus was determined by tabulating the average top-peak to bottom-peak magnitude for a given sinusoidal stress response, and dividing it by the same average value for the corresponding applied sinusoidal shear strain. Thus the dynamic shear modulus is

$$G = \frac{|\tau|}{|\gamma|}. \quad (4)$$

### 3.3 Results

The hydrogel constructs exhibited a stress-relaxation response to the application of ramp shear strains at a rate of 50  $\mu\text{m}/\text{sec}$ . The equilibrium modulus was obtained by applying successive shear strain ramps and taking the slope of the relaxation stress values for each strain magnitude. An example of the stress-strain response of a sample at Day 30 is shown in Figure 9. At early time points, the shear stress was not linearly correlated with shear strain and appeared to be random. However, at later time points, some as early as Day 15 and consistently by Day 30, the constructs developed a linear stress-strain relationship, corresponding to an average equilibrium modulus of  $5.2 \pm 2$  kPa. The equilibrium modulus of cartilage at the same ionic concentration has been reported to be  $\sim 375$  kPa [58]. Similar to the relaxed stress, the equilibrium peak stress was linear with strain magnitude at Day 30, but randomly correlated at earlier time points (Figure 10). The hydrogel equilibrium modulus increased over time (Figure 11), with a maximum recorded average of  $\sim 8 \pm 1$  kPa at Day 35.

In response to applied dynamic strain, the phase lag between stress and strain demonstrated a viscoelastic quality (Figure 12). As with the equilibrium modulus, the dynamic modulus also increased with time, reaching a maximum average value of  $67.7 \pm 21$  kPa at Day 35 (Figure 13). Comparatively, cartilage explants had a dynamic modulus of  $\sim 1.5$  MPa for the same ionic concentration [58]. In the nature of viscoelastic materials, the dynamic stress response was dependent on strain frequency and amplitude. However, only data from the 0.5 Hz frequency and 0.8% amplitude are shown here.

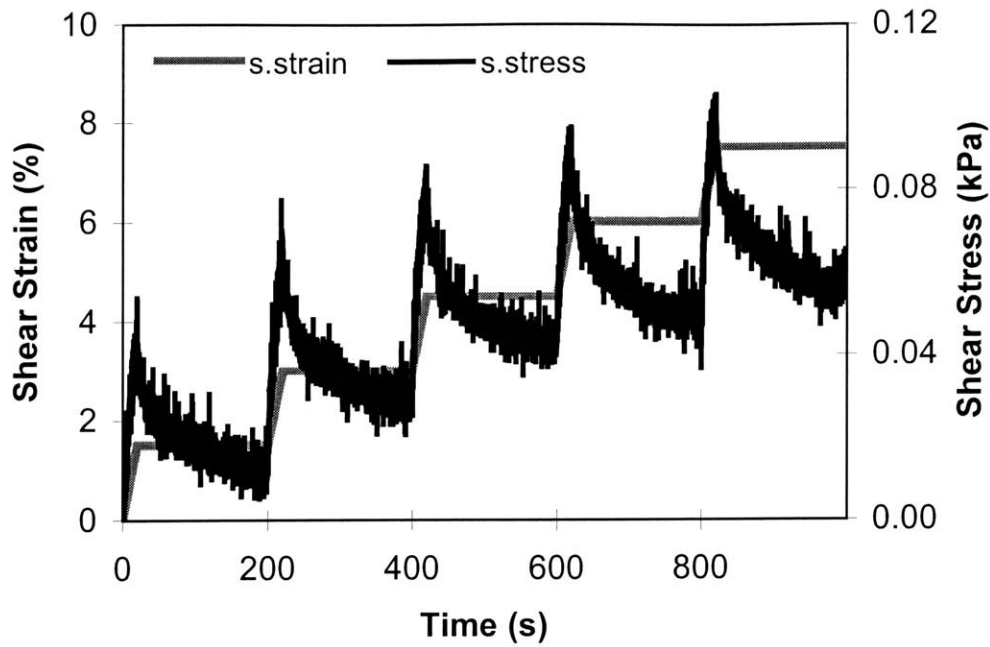


Figure 9: The intrinsic time-dependent stress relaxation response of a 30-day-old construct to successively applied ramp-and-hold shear strains.

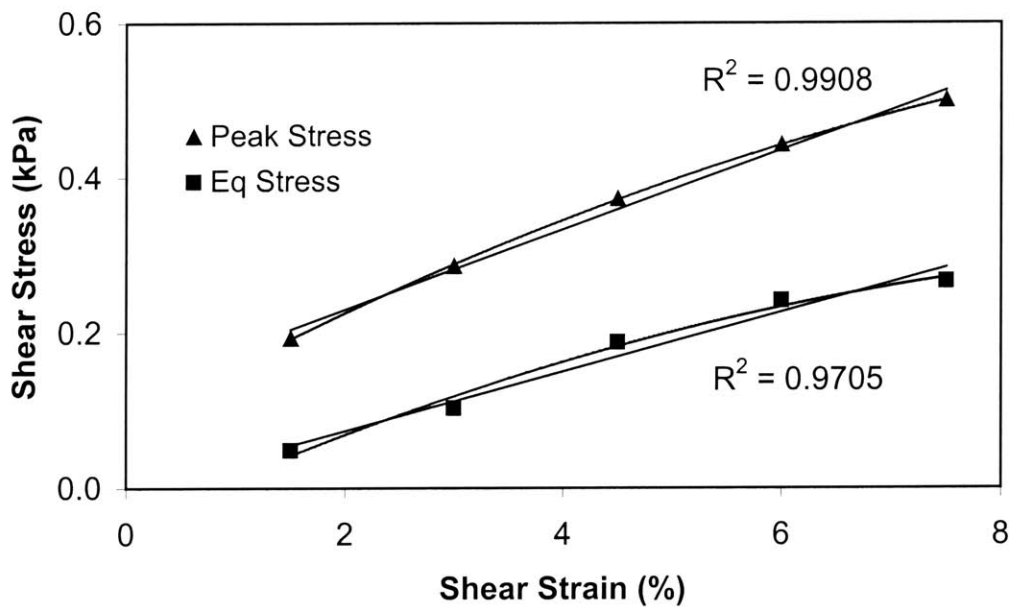


Figure 10: The peak and equilibrium shear stress of 30-day-old constructs in response to ramp-and-hold shear strain. Both the peak and equilibrium shear stresses show a linear correlation with shear strain, with linear regression  $R^2$  values of 0.99 and 0.97, respectively.



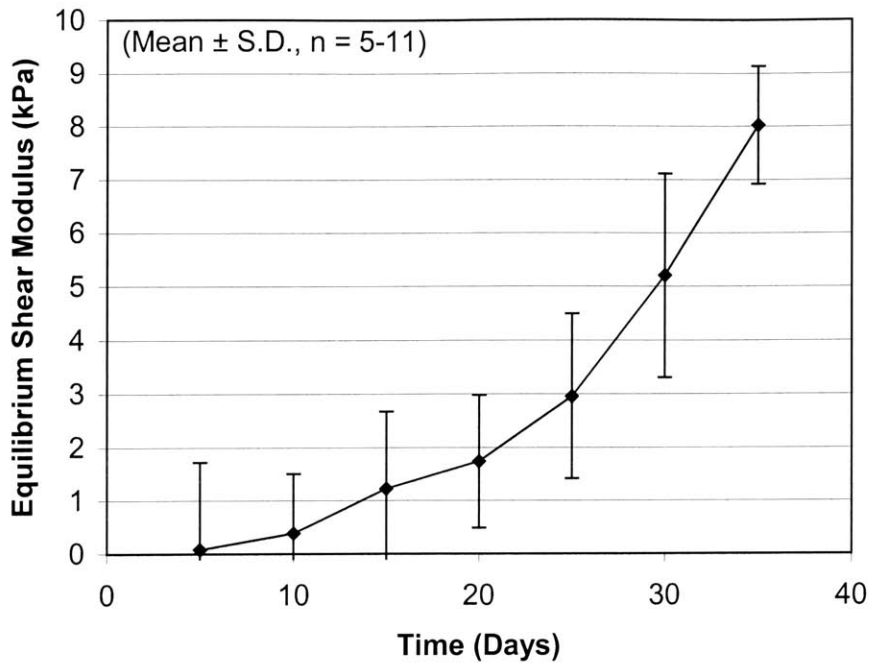


Figure 11: The average equilibrium shear modulus of constructs over time (n=5-11). From Day 5 to Day 35, the modulus increased to  $5.2 \pm 2$  kPa.

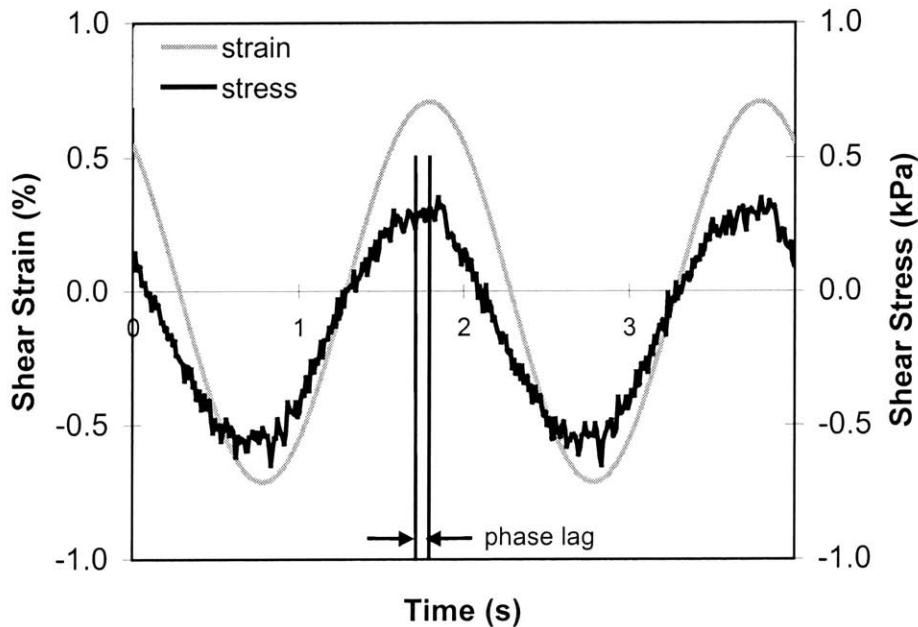
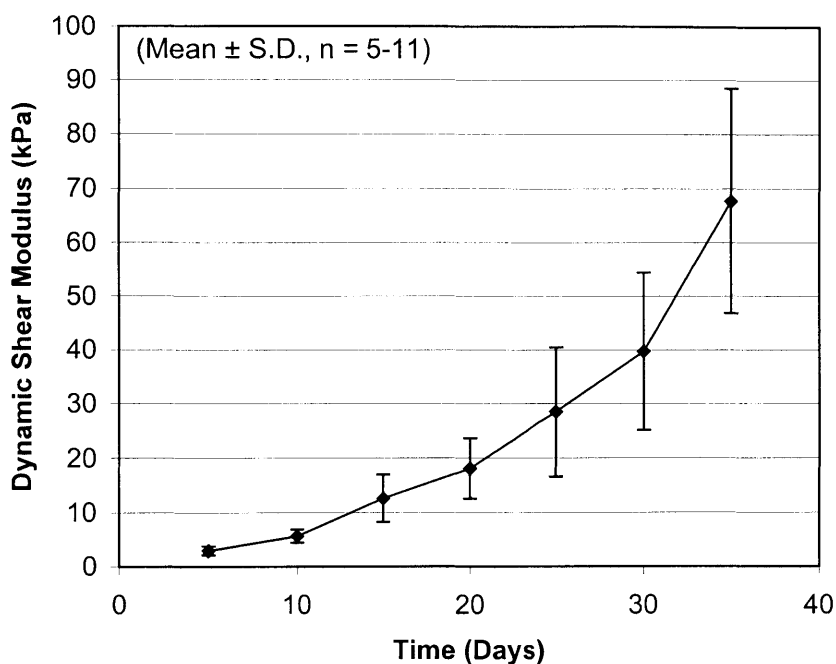


Figure 12: A representative shear stress response of constructs to applied sinusoidal shear strain at 0.5 Hz. The  $\sim 17$  degree difference in phase angle the between stress and strain curves demonstrates the viscoelastic behavior of the material, with elasticity being dominant over viscous effects.



**Figure 13:** The average dynamic shear modulus of constructs over time (n=5-11). From Day 5 to Day 35, the modulus increased to  $67.7 \pm 21$  kPa.

### 3.4 Discussion

The equilibrium and dynamic shear properties of chondrocyte-seeded, self-assembling peptide hydrogels over time were determined via the application of torsional, pure shear loading. The material exhibited viscoelastic behavior in response to both equilibrium and dynamic shear deformation. When a shear ramp was applied, the response was a stress-relaxation curve, attesting to the porous, multi-compositional nature of the material. Stress equilibrium was reached after approximately 2-4 minutes in 30-day-old specimens, compared to 6-10 minutes in explants [58]. A lower density of extracellular matrix molecules in these hydrogels may explain their lower relaxation time constant. As with cartilage explants, the hydrogel stress response to dynamic shear strain was dependent on both frequency and strain amplitude, although only the data for 0.5 Hz and 0.8% amplitude are presented here. Furthermore, the response to sinusoidal shear deformation showed a stress-strain phase difference of approximately 17 degrees at Day

30, similar to a 5-25 degree difference in cartilage [58, 59]. This phase shift value was consistent among all samples tested at that age. As previously reported, a perfectly elastic material would produce a stress response that is in phase with the applied sinusoidal strain, whereas a perfectly viscous liquid would produce a 90 degree phase shift for the same strain [76]. Therefore, the hydrogel constructs in this study have a combination of elastic and viscous qualities, the former being more dominant and probably resulting from spring-like energy storage in deformed extracellular matrix molecules. The viscous effects manifest energy dissipation, which previous investigators have proposed is a result of frictional interactions between proteoglycan, collagen, and water in cartilage [59]. Since fluid flow can be neglected in this experiment, inter-proteoglycan, inter-collagen, and proteoglycan-collagen interactions are likely to be the sources of viscous dissipation.

As expected, the shear material properties of chondrocyte-seeded KLD-12 hydrogels were time-dependent, based on measurements taken from Day 5 to Day 35 after casting. Both the equilibrium and dynamic moduli increased over time, reflecting the continuous accumulation of newly synthesized extracellular matrix molecules within the hydrogel scaffolds. This phenomenon may explain why both the peak and equilibrium shear stress values were randomly correlated with increasing shear strains at early time points, but developed a linear correlation by Day 30, and as early as Day 15 in some specimens. At Day 35, the equilibrium and dynamic stiffnesses were still several orders of magnitude lower than the corresponding material properties of cartilage explants at the same ionic concentration [58, 77]. This is likely due to lower protein and proteoglycan content and higher water content in the hydrogels at this age. Additionally, the random orientation of collagen fibers in the hydrogels, compared to a more structured orientation in explants may have also contributed to their lower shear stiffness. Hydrogel shear moduli were also much lower than compressive moduli of the same material, measured by Kisiday et al. [22, 24], because confined compression of the material would result in added stress resistance due to hydrostatic pressure, which is lacking in shear deformation.

## **Chapter 4**

# **Effect of Dynamic Shear Loading on Chondrocyte Metabolism**

### **4.1 Introduction**

There is much evidence to support the theory that mechanical forces play a crucial role in the development and maintenance of biological tissues. This is certainly the case in articular cartilage, which experiences a wide variety of physiological forces and is a biomechanically and electrochemically complex tissue [64]. Investigators have utilized the knowledge that mechanical forces are coupled to chondrocyte metabolism in attempts to engineer better artificial versions of the tissue. Several kinds of tissue-engineered cartilage have responded positively to dynamic loading [16, 18, 45, 62]. Specifically, Kisiday et al. developed a novel, alternate-day, intermittent, dynamic compression protocol to stimulate proteoglycan synthesis and promote its retention within chondrocyte-seeded KLD-12 hydrogels [21, 24]. The specific loading pattern that was employed in those studies was derived from dynamic compression schemes that have induced similar results in cartilage explants and chondrocyte-seeded agarose hydrogels [20, 60, 61, 64]. Similarly, this thesis aimed to reproduce in seeded KLD-12 hydrogels the dynamic shear-induced stimulation of both protein and proteoglycan synthesis that was seen in cartilage explants [35, 57]. Other studies demonstrating that dynamic shear

deformation stimulated biosynthesis in cartilaginous tissue formed *in vitro* [62, 63] encourage the hypothesis that the same phenomenon could apply to KLD-12 constructs.

The shear loading parameters selected for the experiments here were based on those previously used in both the explant shear and the KLD-12 hydrogel compression studies. The chosen loading frequencies, magnitudes, and duty cycles are those that induced the greatest augmentation of biosynthesis in the afore-mentioned studies. A new culture chamber was designed and manufactured to accommodate shear and compressive loading of 12.5 mm diameter hydrogel disks. It is a hybrid of existing chambers for compression and shear applied by an incubator-housed loading apparatus [24, 57], combining the well size of the former with the shear capabilities of the latter.

## **4.1 Methods**

### **4.1.1 Development of Shear Loading Chamber for Hydrogel Disks**

A new polysulfone (PSF) bioreactor for shear loading was designed and machined (Figure 14). The critical design parameters were large wells to accommodate 12.5 mm diameter hydrogel disks; adjustable-height, porous, polyethylene (HDPE, Porex Corp., Fairburn, GA) platens to adjust for varying sample thickness and to allow nutrient diffusion during contact; cone-point set screws for securing the platens at a desired height without laterally shifting them; a shear attachment, with which to fix the lid to the Incudyn for axial movement; an internal geometry such that when the platens were fully raised and the lid was resting on the base, there were no contact stresses on the hydrogels.

Several validation tests were run to ensure that each adjustable platen was evenly contacting the surface of its corresponding hydrogel. Different numbers and distributions of hydrogels were placed in the chamber wells, and the platens were dropped, tightened, and zeroed. In each trial configuration, a compressive ramp was issued, and the waveform stress response was examined for any inconsistencies that would signify uneven surface contact. The drop-down system was found to be accurate within  $\pm 25 \mu\text{m}$  of the sample surface, which was considered to be an acceptable tolerance.

The polysulfone chamber base, lid, and screw components could be sterilized by autoclaving. However, autoclaving of the HDPE platens caused them to warp slightly and loosen from their PSF holders. Therefore, the platens and their holders were ethanol sterilized and thoroughly rinsed with PBS prior to specimen contact.

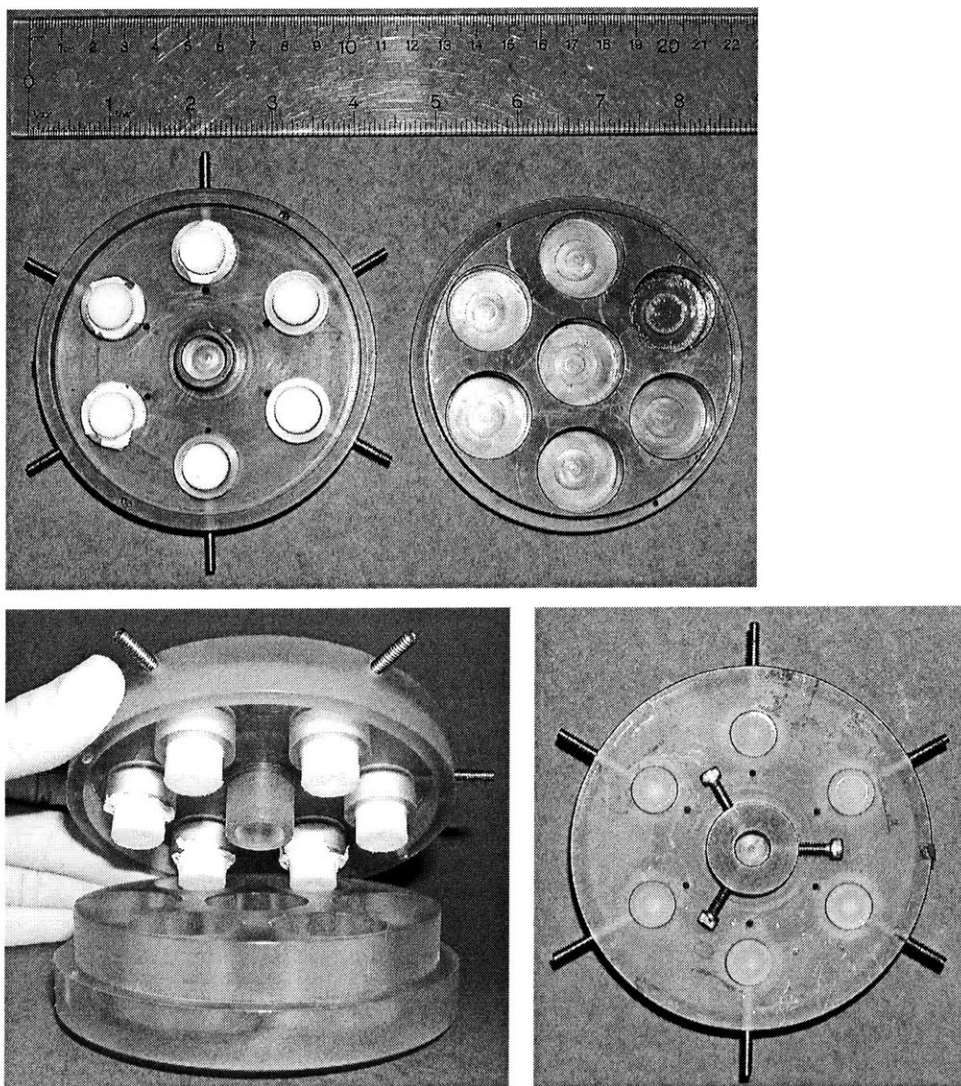


**Figure 14:** A new shear polysulfone chamber for shear loading of the constructs. Notable features include adjustable-height porous platens, large well size, and top shear-axel attachment.

#### 4.1.2 Shear Loading

Chondrocyte-seeded KLD-12 hydrogels were transferred to individual wells of the shear loading chamber, and the lid was placed on top, such that there was no contact

between the hydrogels and the loading platens. Low-serum medium (see Chapter 2) was supplied to each occupied well via syringe injection through 0.625 in diameter feedholes in the lid. To preserve sterility within the chamber, two layers of gauze were lightly soaked with ethanol and wrapped around the circumference of the chamber, covering the gap between the base and the lid, and gauze pieces were stuffed into the feedholes. The adjustable platens were then released to lightly rest on the hydrogel surfaces, keeping the hydrogels centered in the wells while the chamber was positioned in the Incudyn (Figure 15). The axially actuated Incudyn post was lowered into the shear lid attachment and fixed to it with set screws. An axial and rotational zero position was established by raising the lid approximately 800  $\mu\text{m}$ , at which each platen, still resting on its corresponding hydrogel surface, was tightened in place. Free-swell control disks were present both in the shear chamber and in a 12-well culture plate, which was placed in the incubator, adjacent to and at the same height as the Incudyn platform.

Beginning with the platens at absolute zero, a 5 or 10% compressive offset was applied, followed by the dynamic shear protocol. Several different shear sequences were tried and their parameters are listed in Table 1, including the amplitude of sinusoidal shear displacement, the dynamic shear frequency, the duty cycle of loading, the hydrogel age at the start of loading, and the types of free-swell controls used. During a rest period in the duty cycle, the platens were raised to approximately 800  $\mu\text{m}$  above zero, so that the samples were in free-swelling. For the necessary protocols, culture medium was changed every other day. At the start of the final 24 hours of the protocol, radiolabel medium containing 10  $\mu\text{Ci/ml}$  of  $^{35}\text{S}$ -sulfate and 20  $\mu\text{Ci/ml}$  of  $^3\text{H}$ -proline was fed to the specimens. At the end of this period, all samples were removed for biochemical analysis.

**Table 1. Dynamic shear loading protocols.**

Protocol	Amp. (%)	Freq. (Hz)	Duty Cycle (hours:minutes)	Age (days)	Free-swell Control
A	2	0.1	0:30 on. 23:30 off. 24:00 rest	14	chamber & 12-well
B	2	0.1	4 x (0:15 on. 5:45 off). 24:00 rest	20	chamber
C	2.5	0.3	4 x (0:45 on. 5:15 off). 24:00 rest	27. 24	chamber & 12-well
D	2.5	0.3	2 x (0:45 on. 5:15 off. 24:00 rest)	34	chamber & 12-well

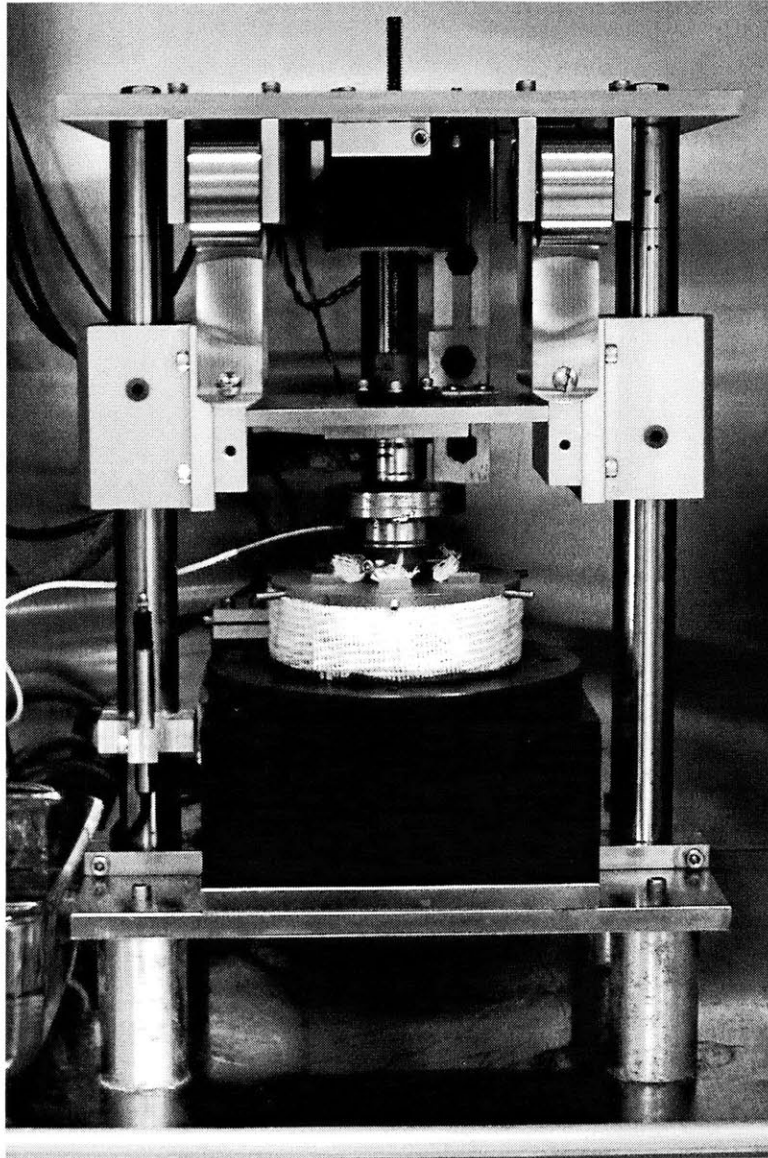


**Figure 15:** The incubator-housed loading apparatus for the precise application of compression and shear. The shear chamber containing tissue constructs is wrapped to preserve sterility and mounted on the Incudyn.

### **4.1.3 Biochemical Analysis**

After various loading protocols, the hydrogel specimens were washed four times in a radiolabel rinse, consisting of 1x PBS and 1 mM unlabeled proline and sulfate to remove all unincorporated radiolabel, after which disk wet weights were recorded. Six to seven 3 mm diameter plugs were then extracted from each 12.5 mm diameter hydrogel



disk, wet weight measured, and digested overnight in 1 ml of proteinase K (Roche) and Tris-HCl solution at 60 °C. Radiolabel incorporation levels of each sample digest were analyzed using a scintillation counter and normalized to plug wet weight. Culture medium from each hydrogel was subjected to a colorimetric DMMB dye assay to assess the amount of GAG loss from the sample. These readings were normalized to the wet weights of corresponding hydrogel disks.

## 4.2 Results

Radiolabel incorporation levels of chondrocyte-seeded KLD-12 hydrogels that were subjected to dynamic shear deformation were compared to those of free-swell controls. In all cases, the biosynthesis rates of chamber specimens, both loaded and free-swell, were significantly lower than those of controls in 12-well plates. This effect was present regardless of the chosen compressive offset, shear amplitude, frequency, and loading time. In sheared samples, incorporation of <sup>3</sup>H-proline and <sup>35</sup>S-sulfate respectively ranged from 41-68% and 34-79% of the corresponding levels in 12-well free-swell controls. Representative results from several of these experiments are shown in Figure 16 and Figure 17. Comparison between loaded and chamber free-swell constructs revealed very similar biosynthetic levels, such that neither group was consistently higher or lower than the other.

The amount of GAG lost from sheared hydrogels into their culture medium was compared to that of chamber free-swell and 12-well free-swell samples. In all instances, GAG levels in the medium of sheared samples were 1-3.5 times those of 12-well controls. In the medium of shear chamber free-swell samples, GAG levels ranged from 0.7-5 times those in 12-well control medium.

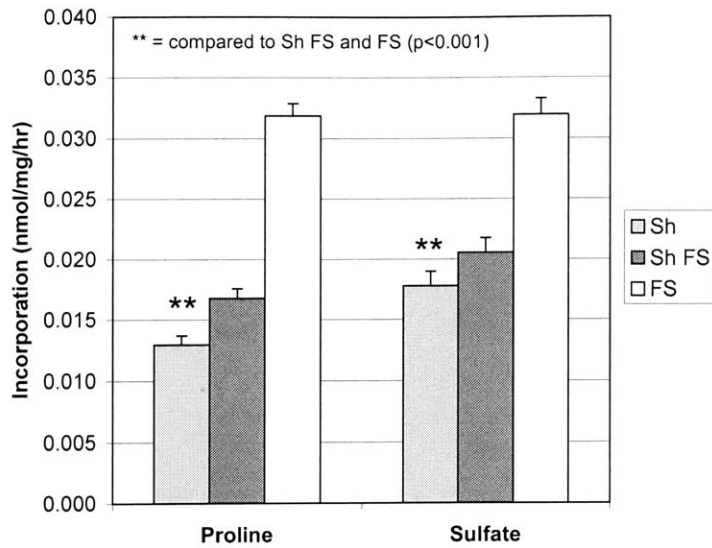


**Figure 16:** The <sup>3</sup>H-proline and <sup>35</sup>S-sulfate incorporation in dynamically sheared (Sh), shear chamber free-swell (Sh FS), and 12-well plate free-swell (FS) constructs. Incorporation in sheared samples was significantly lower (p < 0.001) than in both other groups.

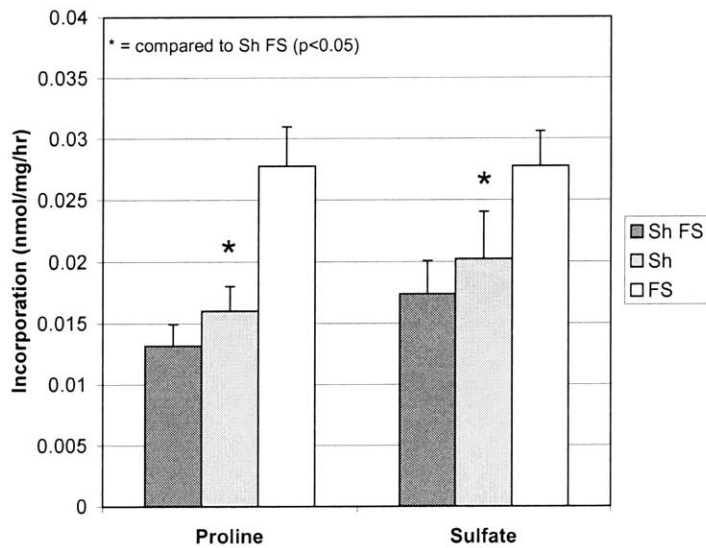


**Figure 17:** The <sup>3</sup>H-proline and <sup>35</sup>S-sulfate incorporation in dynamically sheared (Sh), shear chamber free-swell (Sh FS), and 12-well plate free-swell (FS) constructs. Compared to chamber free-swell, incorporation in the sheared disks was significantly higher (p < 0.05), and both of those groups had significantly lower (p < 0.001) incorporation than the 12-well free-swell controls.

### 4.3 Discussion

Physical forces are known to have a significant effect on the metabolism of chondrocytes in many different environments, whether *in vivo* tissue, cartilage explants, monolayer cultures, or tissue engineered constructs [14, 16-20, 24, 35, 57, 62, 63]. While these forces can certainly have a destructive influence, certain modes of dynamic mechanical loading have been shown to enhance biosynthesis of ECM molecules by chondrocytes. Jin et al. demonstrated that dynamic shear loading could stimulate protein and proteoglycan production in cartilage explants [35, 57], while Waldman et al. reported the same effect in cartilaginous tissue formed by *in vitro* chondrocyte cultures [62, 63].

To investigate whether the same biosynthetic enhancement would apply to chondrocyte-seeded KLD-12 hydrogels, they were subjected to various dynamic shear protocols and the radiolabel incorporation of newly synthesized protein and proteoglycan in the constructs was analyzed. In contrast to previous studies, sheared specimens showed a dramatic decrease in both protein and proteoglycan synthesis, compared to controls in 12-well culture plates. Both the sheared constructs and the 12-well controls exhibited slightly higher proteoglycan incorporation over protein incorporation, although occasionally in shear samples, neither matrix component had a significantly higher incorporation rate than the other.

The shear loading parameters applied to the hydrogel constructs were chosen based on those used in previous shear studies, as well as those used in studies of dynamic compression of seeded KLD-12 hydrogels [24]. They combined low frequencies, low amplitudes, and intermittent loading patterns, which prior research identified as anabolic stimuli. Initially, the suppressed biosynthesis seen in shear constructs was thought to be due to adverse loading parameters. However, the same occurrence in free-swelling constructs in the loading chamber suggested that the biosynthetic repression might have been an artifact of the chamber itself, instead of a side effect of loading. Observation of increased GAG loss to the medium in both loaded and unloaded chamber samples, compared to 12-well controls, supported this new hypothesis and prompted a more thorough investigation of the shear chamber as a suitable environment for hydrogel culture. The details of this spin-off chamber study are described in Chapter 5.

# Chapter 5

## Validation of Polysulfone Loading Chambers

### 5.1 Introduction

Polysulfone (PSF) has been well documented as a suitable material for biological devices, including bioreactors, dialysis machines, and orthopedic implants [16, 57, 65-69]. It has frequently been used to fabricate custom loading chambers for cartilage explants and tissue-engineered cartilage specimens. This precedent justified the decision to machine the new chamber for this thesis out of PSF. In testing, however, samples cultured in the new chamber exhibited a marked decrease in biosynthesis and increase in GAG loss to medium, raising the possibility that the chamber environment was not biocompatible with chondrocyte-seeded KLD-12 hydrogels. Suspected sources for these adverse effects were toxic residues from chamber sterilization processes, improper gas exchange, or harmful agents leaching out of the chamber material.

Validation experiments were performed in an effort to resolve these issues and identify which, if any, was the perpetrator. First, the new chamber was compared to an existing compression chamber of the same material and almost identical internal geometry to determine whether the problem was localized to the new chamber alone, or whether it pertained to other similar PSF chambers as well. Different methods of wrapping the chamber in gauze and Parafilm, as described in Chapter 4, were tested to check whether changes in gas diffusion patterns within the chamber would have significant implications on construct metabolism. When excessive GAG loss and

biosynthetic suppression were found in both chambers, independent of wrapping methods, compared to controls in 12-well culture plates, it was hypothesized that contact with PSF may have been responsible. One explanation was that a soluble factor might have been leaching out of the PSF and affecting chondrocyte metabolism and cytokine release [70]. Thus, sterile chamber wells were extensively washed and rinsed with PBS or FBS prior to hydrogel culture, in attempts to eliminate the offending soluble agents.

This treatment seemed to be ineffective, so a more rigorous approach was taken to sequester samples from direct contact with polysulfone. Chamber wells were coated with Poly(2-Hydroxyethylmethacrylate) (Poly-HEMA) solution, forming a barrier between the sides of the chamber wells and the hydrogels. A thin-walled Teflon (PolyTetraFlouroEthylene, PTFE) “sleeve”, which fit snugly into the chamber well, was machined and tested as another type of PSF-hydrogel barrier. Both Poly-HEMA and Teflon have been documented as biocompatible materials for chondrocyte culture [71 - 73].

## **5.2 Methods**

### **5.2.1 Chamber Comparison**

The shear chamber and a compression chamber with very similar geometry were autoclaved and allowed to cool and dry. Chondrocyte-seeded KLD-12 hydrogels were placed in the wells of each chamber and also in a 12-well culture plate. Each chamber was wrapped with gauze (see Chapter 4) and a strip of ethanol-soaked Parafilm, forming a sterile barrier between base and lid. Both chambers and the 12-well plate were positioned adjacent to each other in the incubator containing the loading apparatus. After 24 hours, the culture medium was replaced with radiolabeled medium. The radiolabel period lasted for another 24 hours, after which all samples were removed, washed, digested, and tested for radiolabel incorporation as described in Chapter 4. Culture medium was saved after each day and analyzed for GAG content (see Chapter 4).

### **5.2.2 Application of Poly-HEME Coating**

A 75% Poly-HEME solution was prepared by adding Poly-HEME crystals to 70% ethanol solution and allowing the mixture to incubate overnight, allowing the crystals to dissolve. This solution was then sterile filtered using a 20  $\mu\text{m}$  syringe filter. Approximately 400  $\mu\text{L}$  of solution was drawn into a pipette and slowly expelled such that it coated all sides of the autoclaved chamber well as evenly as possible. After about 30 minutes the ethanol evaporated and the dry Poly-HEME coating was examined for bare spots. If necessary, a second coating was applied by the same procedure. Hydrogel specimens were then placed in coated and uncoated chamber wells and in a 12-well plate. The chamber was sterilely wrapped and transferred to the incubator along with a 12-well control plate, as previously described. Culture lasted for 2 days, including a change to radiolabel medium for the last 24 hours. As before, radiolabel incorporation of each sample and GAG content of the medium were measured.

### **5.2.3 Use of Teflon Sleeve**

A Teflon “sleeve” (Figure 18) was machined using only water as a cutting coolant. The geometry was such that the thin-walled sleeve fit snugly into a well of the shear chamber. This piece was sterilized by autoclaving. To validate the appropriateness of the sleeve material and environment for culture, a hydrogel was placed in it, supplied with medium, covered with a petri dish lid, and placed in an incubator, alongside a control hydrogel in a 12-well culture plate. In another experiment, the sleeve was inserted into a shear chamber well. The sleeve well, standard well, and 12-well plate were supplied with hydrogels, which were cultured for 2 days and whose digests and media were analyzed as described in the previous two sections.

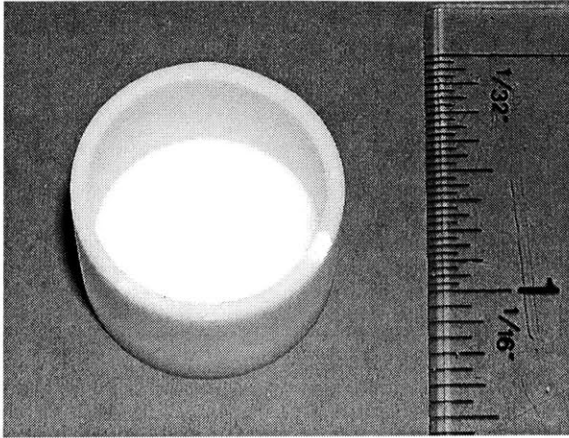


**Figure 18: The Teflon sleeve to be inserted in the polysulfone loading chamber.**

### **5.3 Results**

Biosynthesis and GAG loss of seeded KLD-12 hydrogels cultured in the unmodified shear chamber wells were compared those of samples in the experimental conditions outlined in the previous section. Independent of specific conditions, all samples within the shear chamber had less biosynthesis and more GAG loss than 12-well controls. GAG loss in untreated shear chamber wells was always much higher, sometimes 7-fold, than GAG loss in 12-well control wells. Interestingly, the compression chamber caused the same biosynthetic suppression and increase in GAG loss that was observed in the shear chamber.  $^3\text{H}$ -proline and  $^{35}\text{S}$ -sulfate incorporation rates of specimens in both chambers were approximately 50% lower than those of controls (Figure 19). In fact, protein and proteoglycan incorporation rates in the compression chamber samples were 40-60% lower than those in the shear chamber.

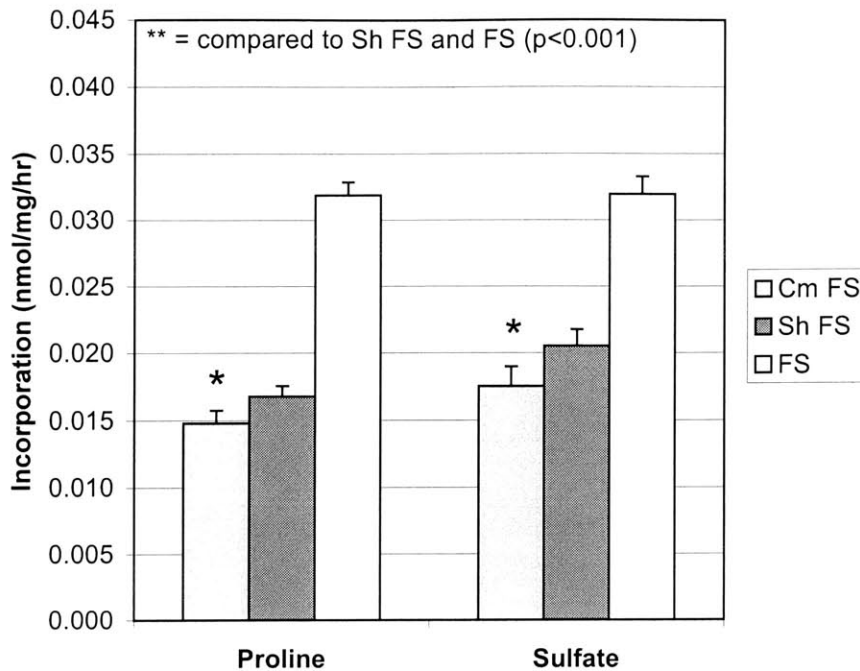


**Figure 19:** The  $^3\text{H}$ -proline and  $^{35}\text{S}$ -sulfate incorporation in compression chamber free-swell (Cm FS), shear chamber free-swell (Sh FS), and 12-well plate free-swell (FS) constructs. Incorporation in the compression chamber was significantly lower ( $p < 0.001$ ) than in the shear chamber, and both were much lower ( $p < 0.001$ ) than controls in the 12-well plate.

Coating the shear chamber wells with Poly-HEME did not significantly influence radiolabel incorporation. There were only slight differences, if any, between coated and uncoated samples, and neither group was consistently higher or lower. Representative radiolabel incorporation data comparing samples in the chamber and 12-well plate, coated and uncoated, is displayed in Figure 20. GAG loss to medium was often curtailed, but not completely eliminated by chamber coating. Although GAG loss in coated wells could be as much as 70% lower than in uncoated wells, it was still 2-3 times higher than in control wells, coated or uncoated after one day in culture (Figure 21). Furthermore, the prevention of GAG loss by coating did not work consistently, and in some cases had no effect.

Radiolabel incorporation levels and GAG loss of samples cultured in the Teflon sleeve alone were not significantly different from those of 12-well controls (Figure 21, and Figure 22). However, samples cultured in the sleeve when it was inserted into the



shear chamber had only slightly higher radiolabel incorporation than those in standard chamber wells (Figure 23). In some cases, GAG loss was half that of uncoated well samples, but still more than twice that of controls (Figure 24).

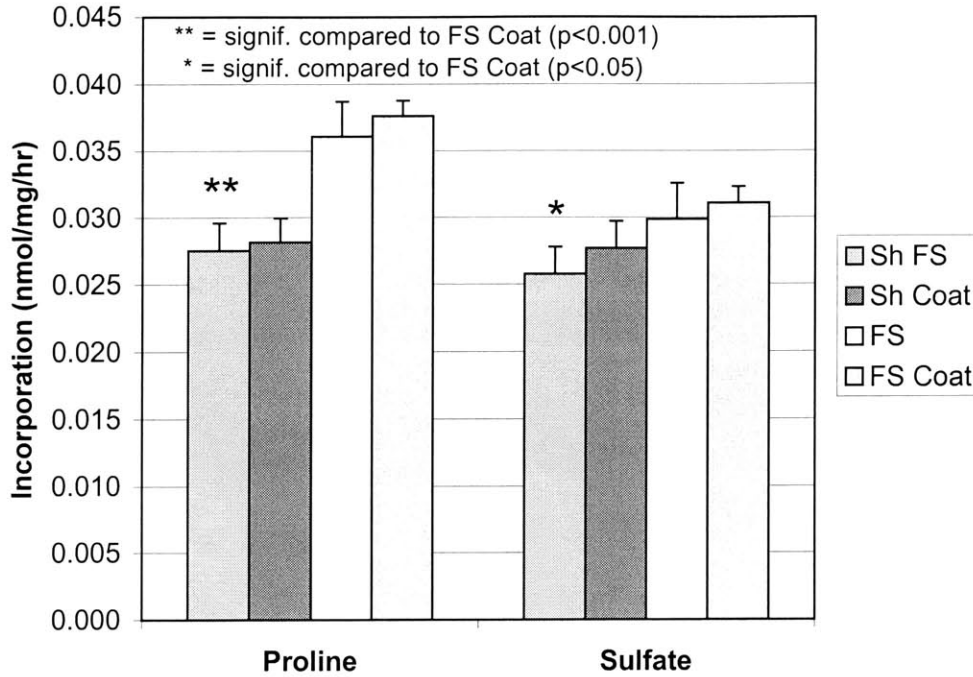


**Figure 20: The <sup>3</sup>H-proline and <sup>35</sup>S-sulfate incorporation in shear chamber free-swell (Sh FS), Poly-HEME-coated shear chamber free-swell (Sh Coat), 12-well plate free-swell (FS), and Ploy-HEME-coated 12-well plate free-swell constructs. Proline and sulfate incorporation levels were slightly lower ( $p < 0.001$  and  $p < 0.05$ , respectively) in uncoated than in coated shear chamber samples. Incorporation in all shear chamber samples was significantly lower ( $p < 0.001$ ) than that in coated and uncoated 12-well controls.**

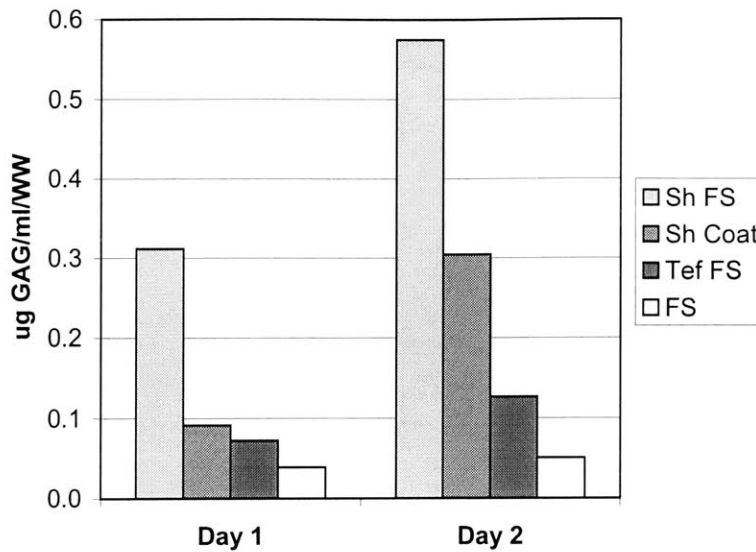


**Figure 21:** The GAG content in the culture medium of shear chamber free-swell (Sh FS), Poly-HEME-coated shear chamber free-swell (Sh Coat), Teflon sleeve free-swell (Tef FS), and 12-well plate free-swell (FS) constructs. After 1 day in culture, shear chamber samples lost approximately 3 times more GAG than coated chamber disks. New medium from the second day in culture contained approximately twice as much GAG in the uncoated than in coated chamber samples. GAG levels in the Teflon sleeve medium remained similar to those of 12-well controls on both days.

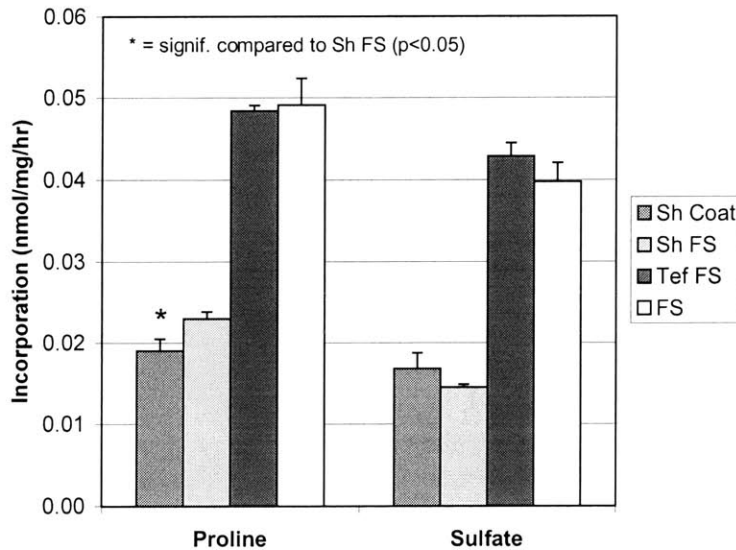


**Figure 22:** The  $^3\text{H}$ -proline and  $^{35}\text{S}$ -sulfate incorporation in Poly-HEME-coated shear chamber free-swell (Sh Coat), shear chamber free-swell (Sh FS), Teflon sleeve free-swell, and 12-well plate free-swell (FS) constructs. Only the proline incorporation in the coated chamber samples was slightly lower ( $p < 0.05$ ) than uncoated; sulfate incorporation levels between the two were not significantly different. Incorporation in Teflon sleeve and 12-well control samples was approximately 2-fold higher than in coated and uncoated chamber samples.

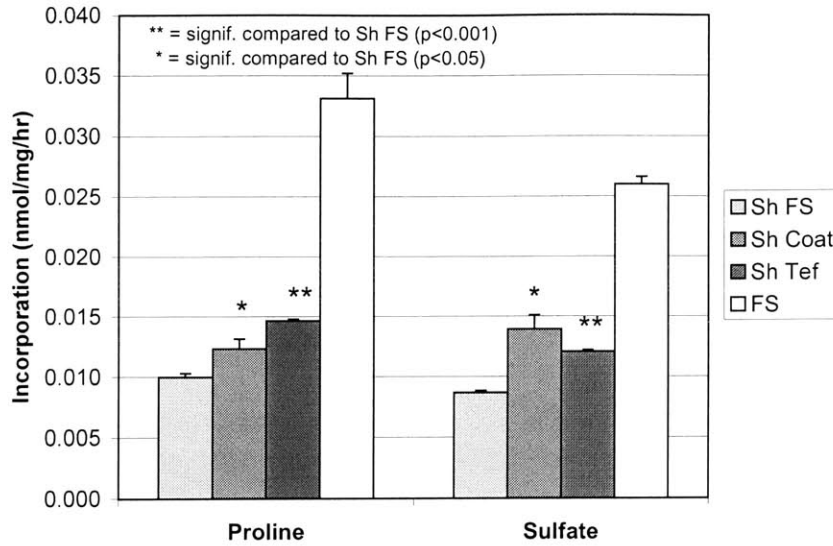


**Figure 23:** The  $^3\text{H}$ -proline and  $^{35}\text{S}$ -sulfate incorporation in shear chamber free-swell (Sh FS), Poly-HEME-coated shear chamber free-swell (Sh Coat), Teflon chamber insert free-swell (Sh Tef), and 12-well plate free-swell (FS) constructs. Incorporation was higher ( $p<0.05$  and  $p<0.001$ , respectively) in both coated chamber and Teflon insert samples, compared to uncoated chamber samples.

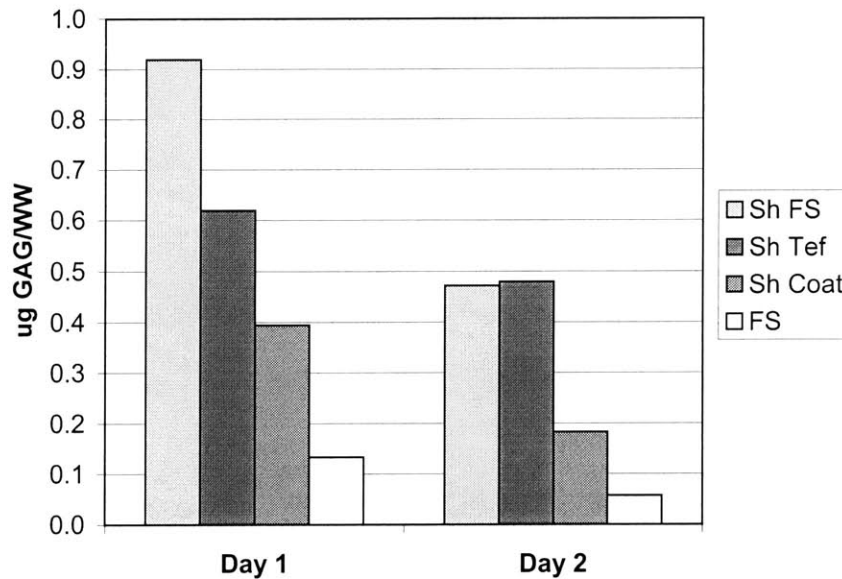


**Figure 24:** The GAG content in the culture medium of shear chamber free-swell (Sh FS), Teflon sleeve free-swell (Tef FS), Poly-HEME-coated shear chamber free-swell (Sh Coat), and 12-well plate free-swell (FS) constructs. After 1 day in culture, chamber free-swell medium had over twice as much GAG as coated-well medium, and ~ 6 times as much as controls. After the second day, all GAG levels were lower, but the ratios between groups remained approximately the same.

## 5.4 Discussion

Polysulfone has extensively been used as a material for a variety of biomedical applications, and numerous researchers have verified its biocompatibility with several tissues and cell types. Bioreactors made of this material have commonly been used for the culture and mechanical stimulation of cartilage explants and tissue-engineered cartilage, and no material incompatibility has been reported [16, 20, 24, 75, 76]. Therefore, the observation that free-swelling chondrocyte-seeded KLD-12 hydrogels cultured in a PSF shear loading chamber had much lower biosynthesis and higher GAG loss than control specimens in a 12-well plate was unexpected. This phenomenon also appeared to be present in another PSF chamber with almost identical geometry to the shear chamber, suggesting that its source was an issue of the chamber environment, not of the shear chamber specifically.

The hypothesis that the PSF was leaching a soluble factor that was adversely affecting chondrocyte biosynthesis and hydrogel GAG retention was not convincing, because neither the Poly-HEME nor the Teflon “barrier” approaches could restore hydrogel activity to control levels. These methods seemed to mitigate the problems, but their action was very inconsistent and unreliable. The Poly-HEME was especially difficult to evaluate, because its coatings were delicate and had a tendency to peel or shrink away from the chamber surface.

Results showing decreased biosynthesis and increased GAG loss in chamber samples, regardless of well treatment, suggest that these artifacts are caused by a factor other than the PSF material, such as altered gas diffusion within the chamber. Higher levels of medium evaporation were noted in the chamber, compared to the 12-well plates, introducing the possibility that there was too much void space within the chamber or that the chamber base and lid were not sufficiently sealed by gauze wrapping. Insertion of the Teflon sleeve into one chamber well also altered the internal space, as it required that the lid be slightly more raised from the lid than usual. Attempts to more securely wrap the chamber, however, did not have a significant effect on hydrogel behavior, so this issue was not satisfactorily resolved.

There remains the question of why PSF culture chambers, such as the shear chamber used in this study, were suitable for cartilage explants, but not for the hydrogel constructs. The inconsistent behavior of free-swelling constructs in the chamber must also be further investigated, as biosynthesis and GAG loss varied widely among experiments.

# Chapter 6

## Summary and Future Work

### 6.1 Summary

These studies are an extension of previous ones, which developed a unique hydrogel construct with promise for tissue-engineering application [15] and which examined the *in vitro* metabolic effects of dynamic loading on cartilaginous tissue specimens [24, 35, 57, 77]. Specifically, a modified version of the chondrocyte-seeded KLD-12 hydrogel construct was developed, as described in Chapter 2, for the purpose of testing its material properties and its metabolic response to dynamic shear deformation. For these uses, a thicker hydrogel than was previously used was advantageous, so the casting equipment and procedure were modified, such that 2 mm thick hydrogel constructs could be fabricated with cell viability comparable to 1.6 mm ones.

To evaluate this construct's potential for implantation *in vivo*, it was necessary to characterize its material properties. The compressive strength of 1.6mm constructs had previously been determined [15], so this study elucidated the shear moduli of 2mm specimens. Chapter 3 discusses how the equilibrium and dynamic moduli were charted over a range of 5 to 35 days after hydrogel casting and both were found to increase dramatically with time, as expected. The material testing protocol was based on a prior one used to evaluate the shear properties of cartilage explants [58]. At early time points, the construct material exhibited a stress-strain response that was, for the most part, random and noisy. However, as the tissue aged, it began to show a viscoelastic stress

response to shear deformation, similar to that of cartilage. By Day 35, the equilibrium and dynamic moduli were still several orders of magnitude lower than those of cartilage explants, but their trends appeared to be climbing.

Dynamic shear loading of the constructs did not produce the hypothesized metabolic side effect (Chapter 4). While certain frequencies and amplitudes of mechanically applied dynamic shear deformation were previously found to increase protein and proteoglycan synthesis in cartilage explants [35, 57, 63], the same effect could not be reproduced in the chondrocyte-seeded hydrogels studied here. In contrast, shear loading of the specimens in a newly designed chamber caused suppression of biosynthesis and increase in GAG loss to the culture medium. This result was unexpected, because similar hydrogel constructs had previously been shown to respond positively to dynamic compression, similar to the way that cartilage explants had [24]. However, an artifact of the loading chamber was suspected to be causing the interference with construct metabolism, because unloaded specimens cultured simultaneously in the chamber experienced the same adverse effects as loaded ones.

Chapter 5 describes how the validity of the shear chamber for hydrogel culture was investigated, in response to the unknown artifact. Although PSF has widely been used as a material for biological culture, these studies questioned its compatibility with seeded KLD-12 hydrogels, considering that two similar culture chambers, the new shear chamber and an existing compression chamber, caused a decrease in biosynthesis and increase in GAG loss in free-swelling samples. Efforts to preserve the internal chamber environment, while eliminating hydrogel contact with any PSF surfaces reduced the problem in some instances, but did not work consistently or completely. The chamber environment itself still seemed to have a dominant deleterious effect on construct homeostasis.

## **6.2 Future Work**

The results in Chapter 3 of this thesis outlined the progression in material properties of chondrocyte-seeded KLD-12 hydrogels over time. However, more in depth

characterization remains to be done, including testing the material behavior at different dynamic strain frequencies and amplitudes. Because these constructs were relatively weak in shear, compared to their compressive stiffness and to shear moduli of cartilage, a more sensitive Incudyn load cell may be required to reduce the noise error in stress measurement at early time points, thus improving the accuracy of extrapolating stiffness values from the data. Similar to studies done on cartilage explants [58], the effect of bath ionic strength on construct stiffness could also be investigated, helping to clarify the individual contributions of proteoglycan and collagen. Furthermore, as a potential candidate for a tissue-engineered implant, the long-term mechanical and biochemical properties of these constructs must be determined. The age limit of constructs presented in this thesis was 35 days in culture. However, investigating a longer time course would be beneficial, especially considering that previous investigators have found shear conditioning of engineered cartilaginous tissue to be effective in the scale of 28-56 days [63].

As explained in Chapters 4 and 5, these studies were unable to determine the reason why the polysulfone shear chamber, in the absence of loading, caused a marked decrease in biosynthesis and GAG retention in the hydrogel constructs. For this reason, it was not clear whether applied deformation or chamber artifacts caused biosynthetic suppression in sheared samples. Further experiments must be done to clarify the mechanism by which this phenomenon occurs. For example, steps could be taken to reduce medium evaporation within the chamber during the culture period, perhaps by adding fluid to empty wells to create moisture “reservoirs”. The chamber could also be modified to reduce the gap between the base and lid. To check whether the effect is present only in PSF chambers with internal geometry for 12.5 mm diameter constructs, 3 mm hydrogel plugs could be cultured, free-swelling, in the shear loading chamber that Jin et al. used for explants. If the chamber problem were solved, loading experiments could be repeated to determine the actual effect of shear deformation on the metabolism of chondrocytes in KLD-12 constructs.

Research on the use of self-assembling peptide hydrogels as scaffolds for chondrocyte encapsulation is still young, and the synthetic nature of these peptides lends them enormous potential for modification to fit a specific tissue-engineering application.



Although beyond the scope of this thesis, testing different amino acid sequences could potentially change casting conditions and improve cell viability within the hydrogel. Biodegradability of the peptides could also be engineered to change the way a construct interfaces with an *in vivo* implant site. Additionally, the use of serum-free medium for construct culture may motivate attempts to tether anabolic growth factors to peptides, altering chondrocyte metabolism and mimicking *in vivo* conditions more closely. These future efforts could improve the effectiveness of self-assembling peptide hydrogels as host environments for chondrocytes and as scaffolds for *in vivo* cartilage repair.

## Appendix A

### Mechanical Drawings of Casting Frame

Figures A-1 and A-2 show schematic drawings of the components of the 2 mm thick hydrogel casting frame. All the dimensions shown are measured in inches.

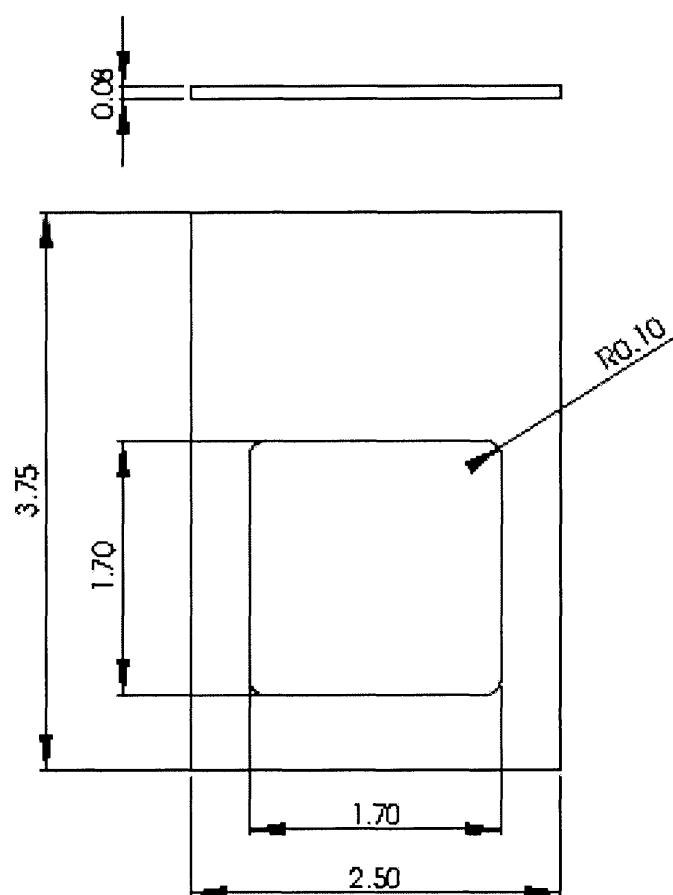
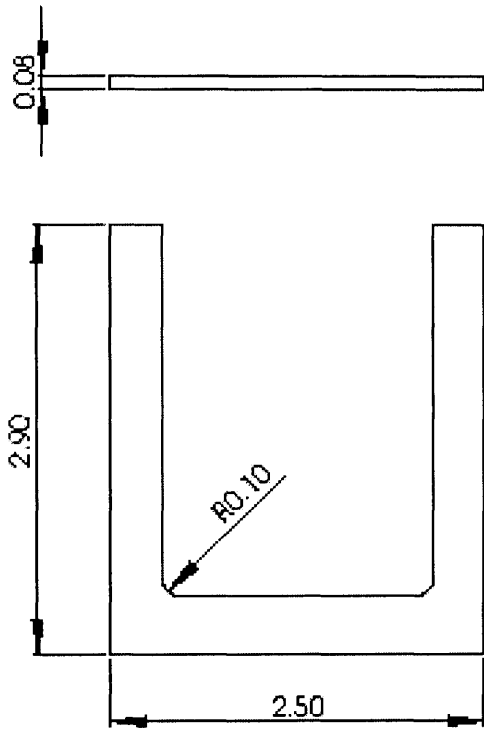


Figure A-1: The casting frame window component, made of stainless steel (quantity 1).



**Figure A-2: The casting frame U-clamp component, made of stainless steel (quantity 2).**

## **Appendix B**

### **Mechanical Drawings of Shear Loading Chamber**

Figures B-1 through B-4 show schematic drawings of the components of the shear loading chamber designed for this thesis. All the dimensions shown are measured in inches.

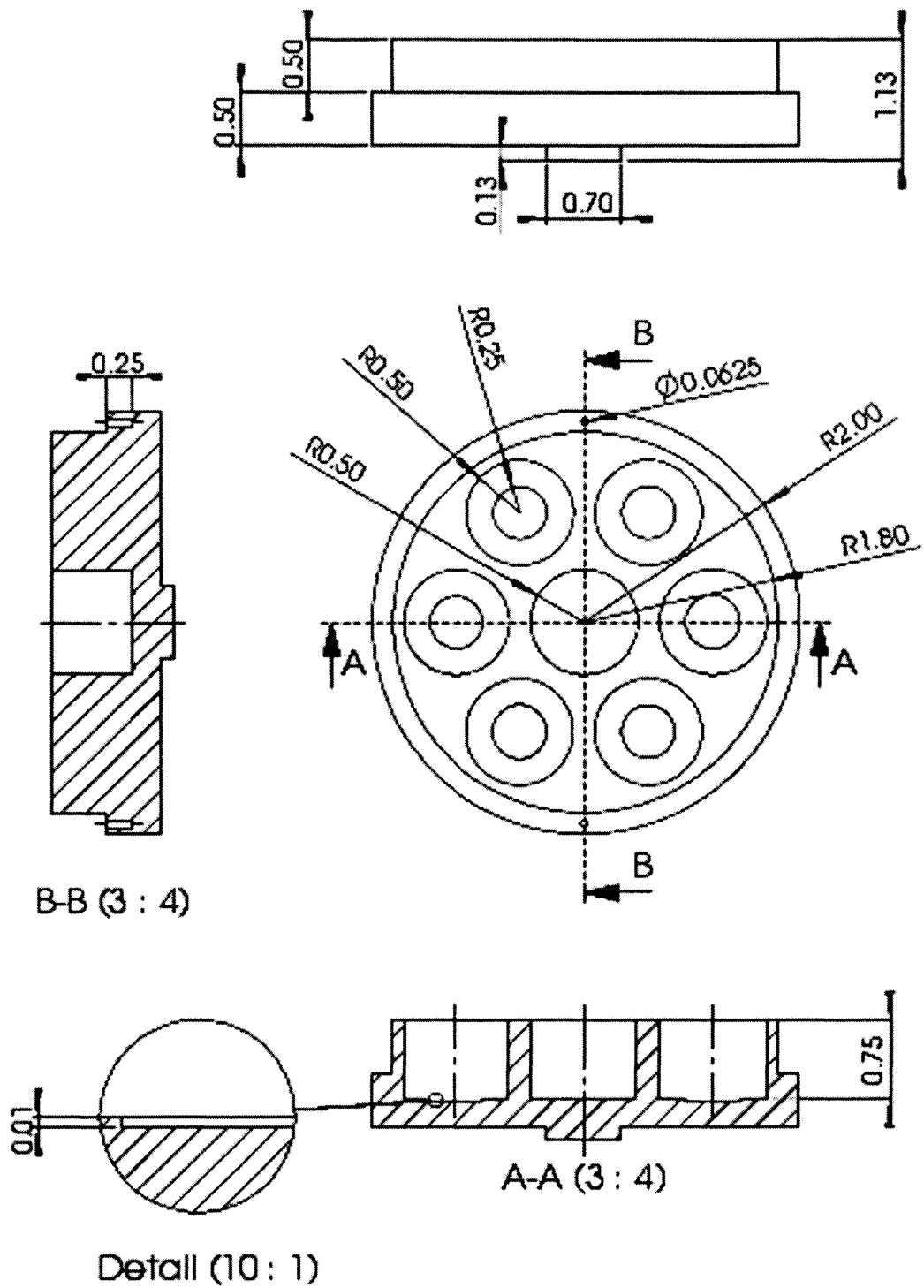


Figure B-1: The shear loading chamber base component, made of polysulfone (quantity 1).

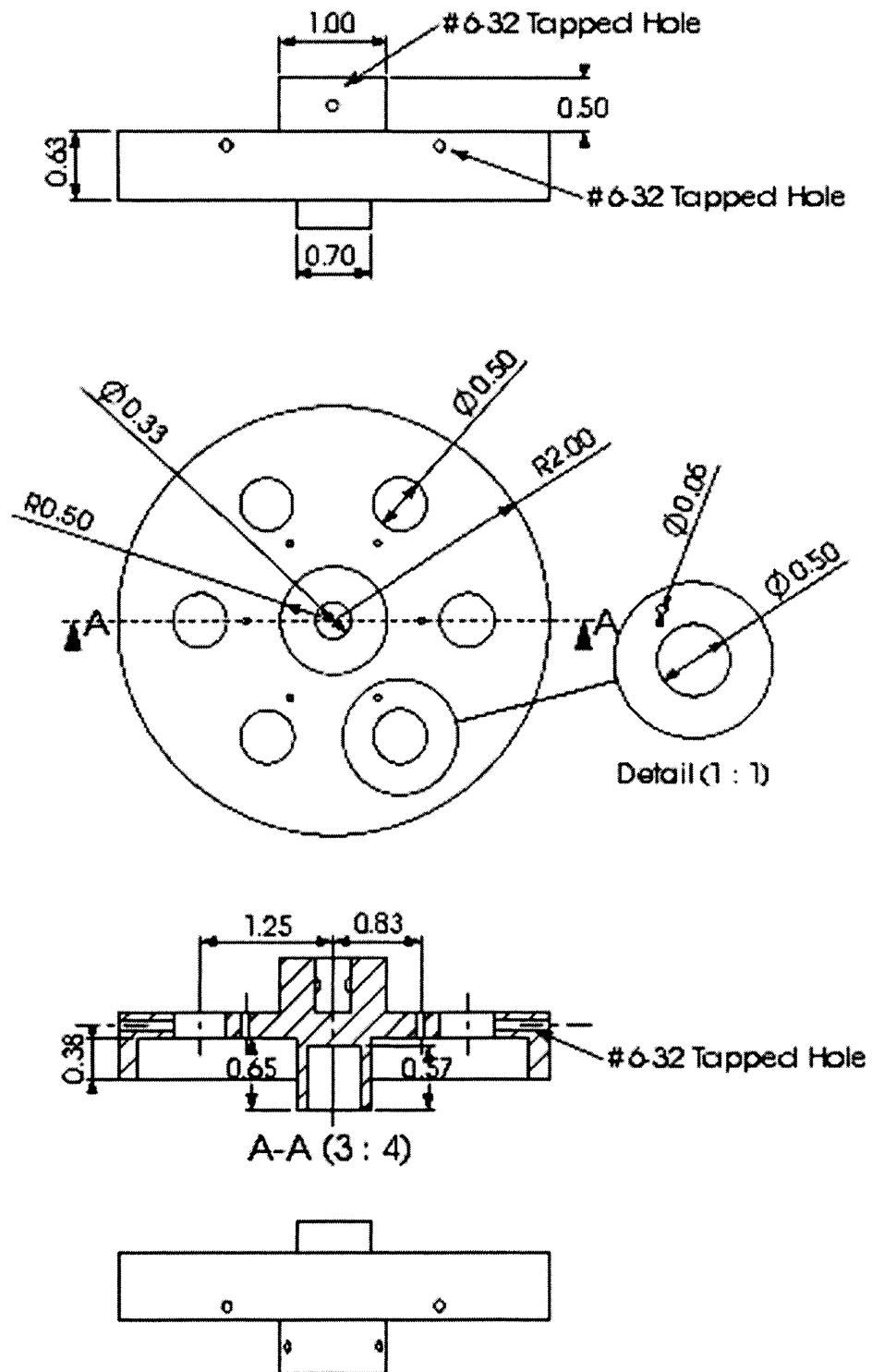


Figure B-2: The shear loading chamber top component, made of polysulfone (quantity 1).

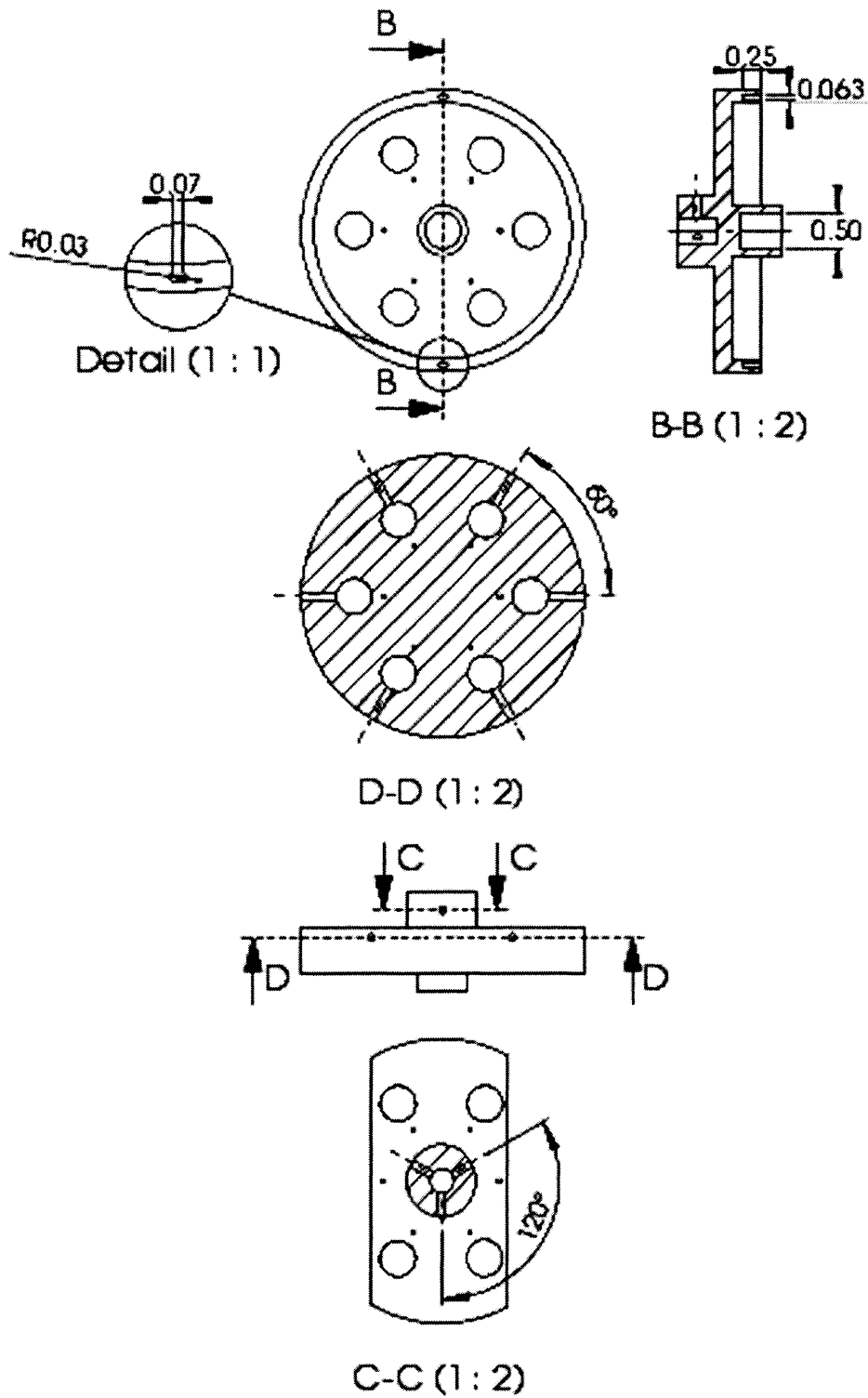


Figure B-3: The alternate view of the shear loading chamber top component shown in Figure B-2.

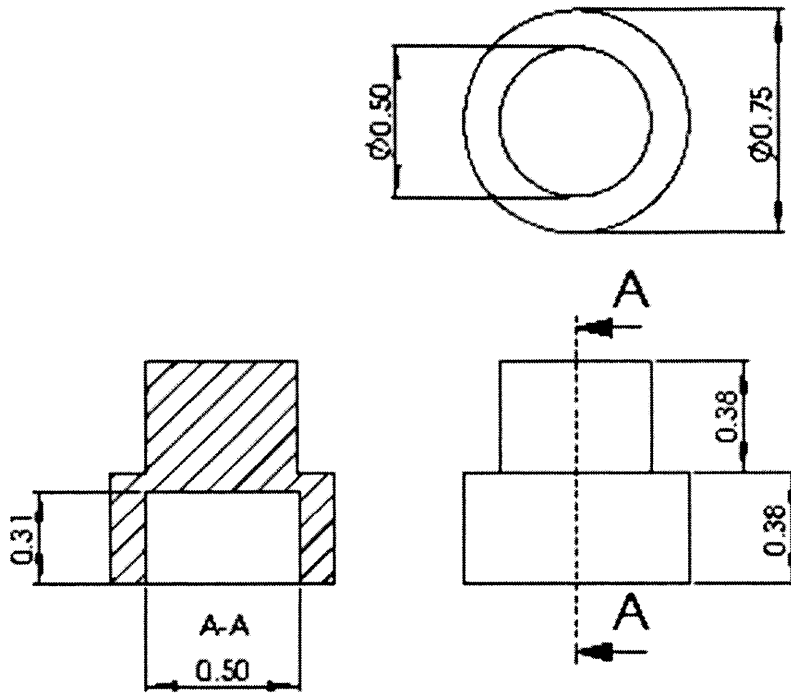


Figure B-4: A polysulfone platen-holder for a porous shear loading platen (quantity 6).



## References

1. Davis MA, Ettinger WH, Neuhaus JM, Cho SA, Hauck WW (1989) The association of knee injury and obesity with unilateral and bilateral osteoarthritis of the knee. *AM J Epidemiol* 130:278-88.
2. Gelber AC, Hochberg MC, Mead LA, Wang NY, Wigley FM, Klag MJ (2000) Joint injury in Young adults and risk for subsequent knee and hip osteoarthritis. *Ann Intern Med* 133:321-8.
3. Rand JA, Trousdale RT, Ilstrup DM, Harmsen WS (2003) Factors affecting the durability of total knee replacement prostheses. *J Bone Joint Surg Am* 85-A(2):259-65.
4. Frenkel SR, Di Cesare PE (1999) Degradation and repair of articular cartilage. *Frontiers in Bioscience* 4:D671-85.
5. Caterson EJ, Nesti LJ, Li WJ, Danielson KG, Albert TJ, Vaccaro AR, Tuan RS (2001) Three-dimensional cartilage formation by bone marrow-derived cell seeded in polylactide/alginate amalgam. *J Biomed Mater Res* 57(3):394-403.
6. Freed LE, Grande DA, Lingbin Z, Emmanuel J, Marquis JC, Langer R (1994) Joint resurfacing using allograft chondrocytes and synthetic biodegradable polymer scaffolds. *Biomed Mater Res.* 28:891-9.
7. Rahfoth B, Weisser J, Sternkopf F, Aigner T, von der Mark K, Brauer R (1998) Transplantation of allograft chondrocytes embedded in agarose gel into cartilage defects of rabbits. *Arthritis Cartilage.* 6(1):50-65.
8. Schaefer D, Martin I, Jundt G, Seidel J, Heberer M, Grodzinsky A, Bergin I, Vunjak-Novakovic G, Freed LE (2002) Tissue-engineered composites for the repair of large osteochondral defects. *Arthritis Rheum.* 46(9):2524-34.

9. Lee CR, Grodzinsky AJ, Hsu HP, Spector M (2003) Effects of a cultured autologous chondrocyte-seeded type II collagen scaffold on the healing of a chondral defect in a canine model. *J Orthop Res.* 21(2):272-81.
10. Sams AE, Nixon AJ (1995) Chondrocyte-laden collagen scaffolds for resurfacing extensive articular cartilage defects. *Osteoarthritis Cartilage.* 3(1):47-59.
11. Nixon AJ, Fortier LA, Williams J, Mohammed H (1999) Enhanced repair of extensive articular defects by insulin-like growth factor-I-laden fibrin composites. *J Orthop Res.* 17(4):475-87.
12. Dausse Y, Grossin L, Miralles G, Pelletier S, Mainard D, Hubert P, Baptiste D, Gillet P, Dellacheria E, Netter P, Payan E (2003) Cartilage repair using new polysaccharidic biomaterials: macroscopic, histological, and biochemical approaches in a rat model of cartilage defect. *Osteoarthritis Cartilage.* 11(1):16-28.
13. Vacanti JP, Langer R (1999) Tissue engineering: the design and fabrication of living replacement devices for surgical reconstruction and transplantation. *The Lancet.* 354:st32-st34.
14. Martin I, Obradovic B, Treppo S, Grodzinsky AJ, Langer R, Freed LE, Vunjak-Novakovic G. (2000) Modulation of the mechanical properties of tissue engineered cartilage. *Biorheology.* 37(1-2):141-7.
15. Kisiday J, Jin M, Kurz B, Hung H, Semino C, Zhang S, Grodzinsky AJ (2002) Self-assembling peptide hydrogel foster chondrocyte extracellular matrix production and cell division: implication for cartilage tissue repair. *Proc Natl Acad Sci.* 99(15):9996-10001.
16. Lee CR, Grodzinsky AJ, Spector M (2003) Biosynthetic response of passaged chondrocytes in a type II collagen scaffold to mechanical compression. *J Biomed Mater Res.* 64A(3):560-9.

17. Mauck RL, Seyhan SL, Ateshian GA, Hung CT (2002) Influence of seeding density and dynamic deformational loading on the developing structure/function relationships of chondrocyte-seeded agarose hydrogels. *Ann Biomed Eng.* 30(8):1046-56.
18. Mauck RL, Soltz MA, Wang CC, Wong DD, Chao PH, Valhmu WB, Hung CT, Ateshian GA (2000) Functional tissue engineering of articular cartilage through dynamic loading of chondrocyte-seeded agarose gels. *J Biomech Eng.* 122(3):252-60.
19. Lee DA, Bader DL (1997) Compressive strains at physiological frequencies influence the metabolism of chondrocytes seeded in agarose. *J Orthop Res.* 15(2):181-8.
20. Buschmann MD, Gluzband YA, Grodzinsky AJ, Hunziker EB (1995) Mechanical compression modulates matrix biosynthesis in chondrocyte/agarose culture. *J Cell Sci.* 108:1497-508.
21. Kisiday J, Jin M, Grodzinsky A (2002) Effects of dynamic compressive loading on in vitro conditioning of chondrocyte-seeded peptide and agarose scaffolds. "48<sup>th</sup> Annual Meeting, Orthopaedic Research Society" [Podium Presentation].
22. Kisiday J, Jin M, Hung H, Kurz B, Zhang S, Grodzinsky A (2001) Self-assembling peptide scaffold for cartilage tissue engineering. "47<sup>th</sup> Annual Meeting, Orthopaedic Research Society" [Podium Presentation].
23. Kisiday J, Siparsky P, Grodzinsky AJ (2003) Anabolic and catabolic response to dynamic compression in a chondrocyte-seeded self-assembling peptide hydrogel. "49<sup>th</sup> Annual Meeting, Orthopaedic Research Society" [Podium Presentation].
24. Kisiday J (2003) In vitro culture of a chondrocyte-seeded peptide hydrogel and the effects of dynamic compression. PhD thesis, Massachusetts Institute of Technology.

25. Jackson DW, Scheer MJ, Simon TM (2001) Cartilage substitutes: Overview of basic science and treatment options. *J Am Acad Orthop Surg.* 9:37-52.
26. Smeathers JE (1992) Cartilage and joints. In *Biomechanics Materials: A Practical Approach*: Vincent JFV (Ed): New York: Oxford University Press: 99-131.
27. Huster D, Schiller J, Arnold K (2002) Comparison of collagen dynamics in articular cartilage and isolated fibrils by solid-state NMR spectroscopy. *Mag Res Med.* 48:624-32.
28. Meachim G, Stickwell RA (1977) The matrix. In *Adult Articular Cartilage*. Freeman MAR (Ed): London: Pitman: 69-144.
29. Socrate S, Boyce M (2001) A constitutive model for the large strain behavior of cartilage. *ASME Bioeng Conf.* 50:597-8.
30. Maroudas A (1990) Methods in cartilage research. In *Methods in cartilage research*. Maroudas A, Kuetter K (Eds): New York: Academic Press: 211.
31. Maroudas A (1976) Balance between swelling pressure and collagen tension in normal and degenerate cartilage. *Nature.* 260:808-9.
32. Muir H (1995) The chondrocyte, architect of cartilage. *BioEssays.* 17(12):1039-1048.
33. O'Driscoll SW (1998) The healing regeneration of articular cartilage [review]. *J Bone Joint Surg Am.* 80:1795-812.
34. Hunter W (1995) Of the structure and disease of articulating cartilages: 1743 [classic article]. *Clin Orthop.* 317:3-6.
35. Jin M, Emkey GR, Siparsky P, Trippel SB, Grodzinsky AJ (2003) Combined effects of dynamic tissue shear deformation and insulin-like growth factor I on chondrocyte biosynthesis in cartilage explants. *Arch Biochem Biophys.* 414:223-31.

36. Zhang S, Altman M (1999) Peptide self-assembly in functional polymer science and engineering. *React Func Poly.* 41:91-102.
37. Kerin A, Patwari P, Kuettner K, Cole A, Grodzinsky A (2001) Molecular basis of osteoarthritis: biomechanical aspects. *Cell Mol Life Sci.* 59(1):27-35.
38. Marini DM, Hwang W, Lauffenburger DA, Zhang S, Kamm RD (2002) Left-handed helical ribbon intermediates in the self-assembly of  $\beta$ -sheet peptide. *Nano Lett.* 2(4):295-299.
39. Caplan MR, Moore PN, Zhang S, Kamm RD, Lauffenburger DA (2000) Self-assembly of a  $\beta$ -sheet protein governed by relief of electrostatic repulsion relative to van der Waals attraction. *Biomacromolecules.* 1:627-31.
40. Zhang S, Lockshin C, Cook R, Rich A (1994) Unusually stable  $\beta$ -sheet formation in an ionic self-complementary oligopeptide. *Biopolymers.* 34:663-72.
41. Zhang S, Marini DM, Hwang W, Santoso S (2002) Design of nanostructured biological materials through self-assembly of peptides and proteins. *Curr Opin Chem Biol.* 6(6):865-71.
42. Zhang S, Holmes TC, DiPersio CM, Hynes RO, Su X, Rich A (1995) Self-complementary oligopeptide matrices support mammalian cell attachment. *Biomaterials.* 16(18):1385-93.
43. Holmes TC, de Lacalle S, Su X, Liu G, Rich A, Zhang S (2000) Extensive neurite outgrowth and active synapse formation on self-assembling peptide scaffolds. *Proc Natl Acad Sci U S A.* 97(12):6728-33.
44. Caterson EJ, Li WJ, Nesti LJ, Albert T, Danielson K, Tuan RS (2002) Polymer/alginate amalgam for cartilage-tissue engineering. *Ann N Y Acad Sci.* 961:134-8.

45. Domm C, Fay J, Schunke M, Kurz B (2000) [Redifferentiation and dedifferentiated joint cartilage cells in alginate culture. Effect of intermittent hydrostatic pressure and low oxygen partial pressure]. *Orthopade*. 29(2):91-9.
46. Holmes TC (2002) Novel peptide-based biomaterial scaffolds for tissue-engineering. *Trend Biotech*. 20(1):16-21.
47. Mak AF (1986) The apparent viscoelastic behavior of articular cartilage – the contributions from the intrinsic matrix viscoelasticity and interstitial fluid flows. *ASME J Biomech Eng*. 108:123-30.
48. Setton LA, Zhu W, Mow VC (1993) The biphasic poroviscoelastic behavior of articular cartilage: role of the surface zone in governing the compressive behavior. *J Biomech*. 26:581-92.
49. Suh JK, DiSilvestro MR (1999) Biphasic poroviscoelastic behavior of hydrated biological soft tissue. *ASME J Mech*. 66:528-35.
50. Silver FH, Bradica G, Tria A (2002) Elastic energy storage in human articular cartilage: estimation of the elastic modulus for type II collagen and changes associated with osteoarthritis. *Matrix Biol*. 21(2):129-37.
51. Silver FH, Christiansen DL, Snowhill P, Chen Y (2000) Role of storage on changes in the mechanical properties of tendon and self-assembled collagen fibers. *Connect Tissue Res*. 41:155-64.
52. Silver FH, Christiansen DL, Snowhill P, Chen Y, Landis WJ (2000) Role of mineral in elastic storage of energy in turkey tendons. *Biomacromolecules*. 1:180-5.
53. Mow VC, Kuei SC, Lai WM, Armstrong CG (1980) Biphasic creep and stress relaxation of articular cartilage in compression: Theory and experiments. *J Biomech Eng*. 102:73-84.

54. Huang C-Y, Mow VC, Ateshian GA (2001) The role of flow-independent viscoelasticity in the biphasic tensile and compressive responses of articular cartilage. *J Biomech Eng.* 123:410-17.
55. Hayes WC, Mockros LF (1971) Viscoelastic properties of human articular cartilage. *J Appl Physiol.* 31:562-8.
56. Hayes WC, Bodine AJ (1978) Flow-independent viscoelastic properties of articular cartilage matrix. *J Biomech.* 11:407-19.
57. Jin M, Frank EH, Quinn TM, Hunziker EB, Grodzinsky AJ (2001) Tissue shear deformation stimulates proteoglycan and protein synthesis in bovine cartilage explants. *Arch Biochem Biophys.* 395(1):41-8.
58. Jin M, Grodzinsky AJ (2001) Effect of electrostatic interactions between glycosaminoglycans on the shear stiffness of cartilage: A molecular model and experiments. *Macromolecules.* 34: 8330-9.
59. Zhu W, Mow VC, Koob TJ, Eyre DR (1993) Viscoelastic shear properties of articular cartilage and the effects of glycosidase treatments. *J Orthop Res.* 11(6):771-81.
60. Kim YJ, Sah RLY, Grodzinsky AJ, Plaas AHK, Sandy JD (1994) Mechanical regulation of cartilage biosynthetic behavior: physical stimuli. *Arch Biochem Biophys.* 311(1):1-12.
61. Buschmann MD, Kim YJ, Wong M, Frank EH, Hunziker EB, Grodzinsky AJ (1999) Stimulation of aggrecan synthesis in cartilage explants by cyclic loading is localized to regions of high interstitial flow. *Arch Biochem Biophys.* 366(1):1-7.
62. Waldman SD, Spiteri CG, Grynblas MD, Pilliar RM, Hong J, Kandel RA (2003) Effect of biomechanical conditioning on cartilaginous tissue formation in vitro. *J Bone Joint Surg Am.* 85-A Suppl 2:101-5.

63. Waldman SD, Spiteri CG, Grynblas MD, Pilliar RM, Kandel RA (2003) Long-term intermittent shear deformation improves the quality of cartilaginous tissue formed in vitro. *J Orthop Res.* 21(4):590-596.
64. Grodzinsky AJ, Levenston ML, Jin M, Frank EH (2000) Cartilage tissue remodeling in response to mechanical loading. *Annu Rev Biomed Eng.* 2:691-713.
65. Wenz LM, Merritt K, Brown SA, Moet A, Steffee AD (1990) In vitro biocompatibility of polyetheretherketone and polysulfone composites. *J Biomed Mater Res.* 24(2):207-15.
66. Hoenich NA, Woffindin C, Mathews JN, Vienken J (1995) Biocompatibility of membranes used in the treatment of renal failure. *Biomaterials.* 16(8):587-92.
67. Behling CA, Spector M (1986) Quantitative characterization of cells at the interface of long-term implants of selected polymers. *J Biomed Mater Res.* 20(5):653-66.
68. Imai Y, Kuo YS, Watanabe A, Masuhara E (1978) Evaluation of polysulfone as a potential biomedical material. *J Bioeng.* 2(1-2):103-7.
69. Vandersteenhoven JJ, Spector M (1983) Osteoinduction within porous polysulfone implants at extrasosseous sites using demineralized allogeneic matrix. *J Biomed Mater Res.* 17(5):793-806.
70. van Loon JJ, Bierkens J, Maes J, Schoeters GE, Ooms D, Doulabi BZ, Veldhuijzen JP (1995) Polysulfone inhibits final differentiation steps of osteogenesis in vitro. *J Biomed Mater Res.* 29(9):1155-63.
71. Bavaresco VP, de Carvalho Zavaglia CA, de Carvalho Reis M, Malmonge SM (2000) Devices for use as an artificial articular surface in joint prostheses or in the repair of osteochondral defects. *Artif Organs.* 24(3):202-5.



72. Xu JW, Nazzari J, Peretti GM, Kirchoff CH, Randolph MA, Yaremchuk MJ (2001) Tissue-engineered cartilage composite with expanded polytetrafluoroethylene membrane. *Ann Plast Surg.* 46(5):527-32.
73. Suh SW, Shin JY, Kim J, Kim J, Beak CH, Kim DI, Kim H, Jeon SS, Choo IW (2002) Effect of different particles on cell proliferation in polymer scaffolds using a solvent-casting and particulate leaching technique. *ASAIO J.* 48(5):460-4.
74. Ragan PM, Chin VI, Hung HH, Masuda K, Thonar EJ, Arner EC, Grodzinsky AJ, Sandy JD (2000) Chondrocyte extracellular matrix synthesis and turnover are influenced by static compression in a new alginate disk culture system. *Arch Biochem Biophys.* 2000 Nov 15;383(2):256-64.
75. Frank EH, Jin M, Loening AM, Levenston ME, Grodzinsky AJ (2000) A versatile shear and compression apparatus for mechanical stimulation of tissue culture explants. *J Biomech.* 33:1523-7.
76. Ferry JD (1970) Viscoelastic properties of polymers. John Wiley & Sons, Inc.
77. Jin M (1999) Regulation of Cartilage Metabolism by Dynamic Tissue Shear Strain and the Mechanical Characterization of Cartilage. MS thesis, Massachusetts Institute of Technology.
78. Jin G, Sah RL, Li YS, Lotz M, Shyy JY, Chien S (2000) Biomechanical regulation of matrix metalloproteinase-9 in cultured chondrocytes. *J Orthop Res.* 18(6):899-908.